SUPPLEMENTARY INFORMATION FOR

The Analytical Flory Random Coil is a Simple-to-Use Reference Model for Unfolded and Disordered Proteins

Jhullian J. Alston[1,2]*, Garrett M. Ginell*[1,2], Andrea Soranno[1,2], Alex S. Holehouse[1,2,✉]

[1]**Department of Biochemistry and Molecular Biophysics**, Washington University School of Medicine, St. Louis, MO, 63110, USA
[2]**Center for Biomolecular Condensates,** Washington University in St. Louis, St. Louis, MO, 63130, USA

* These authors contributed equally to this work

✉ Corresponding author, e-mail: alex.holehouse@wustl.edu

1. SUPPLEMENTARY METHODS

1.1 Finite size effects as assessed by the Flory characteristic ratio

We assessed finite-size effects for FRC simulations in several ways, comparing against excluded volume (EV) simulations as a real-chain reference model. First, we compared internal scaling profiles. For real chains, residues at or near the ends have a great volume of space they can explore than residues internal to chain due to excluded volume of the chain. This manifests for internal scaling profiles whereby super-imposing a series of homopolymers of different lengths reveals the distance between residue 1 and n when 1 and *n* are the first and terminal residues is shorter than residue 1 and n when n is an internal residue (**Fig. 1E**). In contrast, because FRC simulations lack any excluded volume contribution, there is no difference between internal and external residues, such that all inter-residue distances of the same residue spacing are equivalent, regardless of where in the chain the two residues lie. This is even more clearly shown by calculating the normalized distance for different inter-residue spacing as a function of starting residue (**Fig. S2C, D**).

The Flory characteristic ratio as;

$$C_n = \frac{\langle R^2 \rangle}{nl^2} \tag{1}$$

Where n is the number of residues, l is the monomer size, and $\langle R^2 \rangle$ is the ensemble-average squared end-to-end distance (or inter-residue distance)[29].

Given both the FRC and AFRC models describe ideal chains, we can empirically define l as using the standard ideal chain relationship;

$$l = \sqrt{\frac{\langle R^2 \rangle}{n}} \qquad (2)$$

in the limit of n tending to ∞[29].

By defining l empirically from our FRC simulations or AFRC model, finite size effects emerge upon plotting n vs. C_n (**Fig. S2E,F**). In FRC simulations, C_n is less than 1 for shorter chains. This is expected in that the rotational isomeric state means local chain geometry is not truly ideal but instead limited to the inter-residue vector path defined by the Ramachandran isomeric states. In contrast, the AFRC is a true ideal chain model, such that the Flory characteristic ratio is always 1 regardless of n. This difference between the AFRC and FRC models manifests as a very slight (1-2 Å) difference in intramolecular distances visible in **Fig. 2A**.

2. SUPPLEMENTARY FIGURES
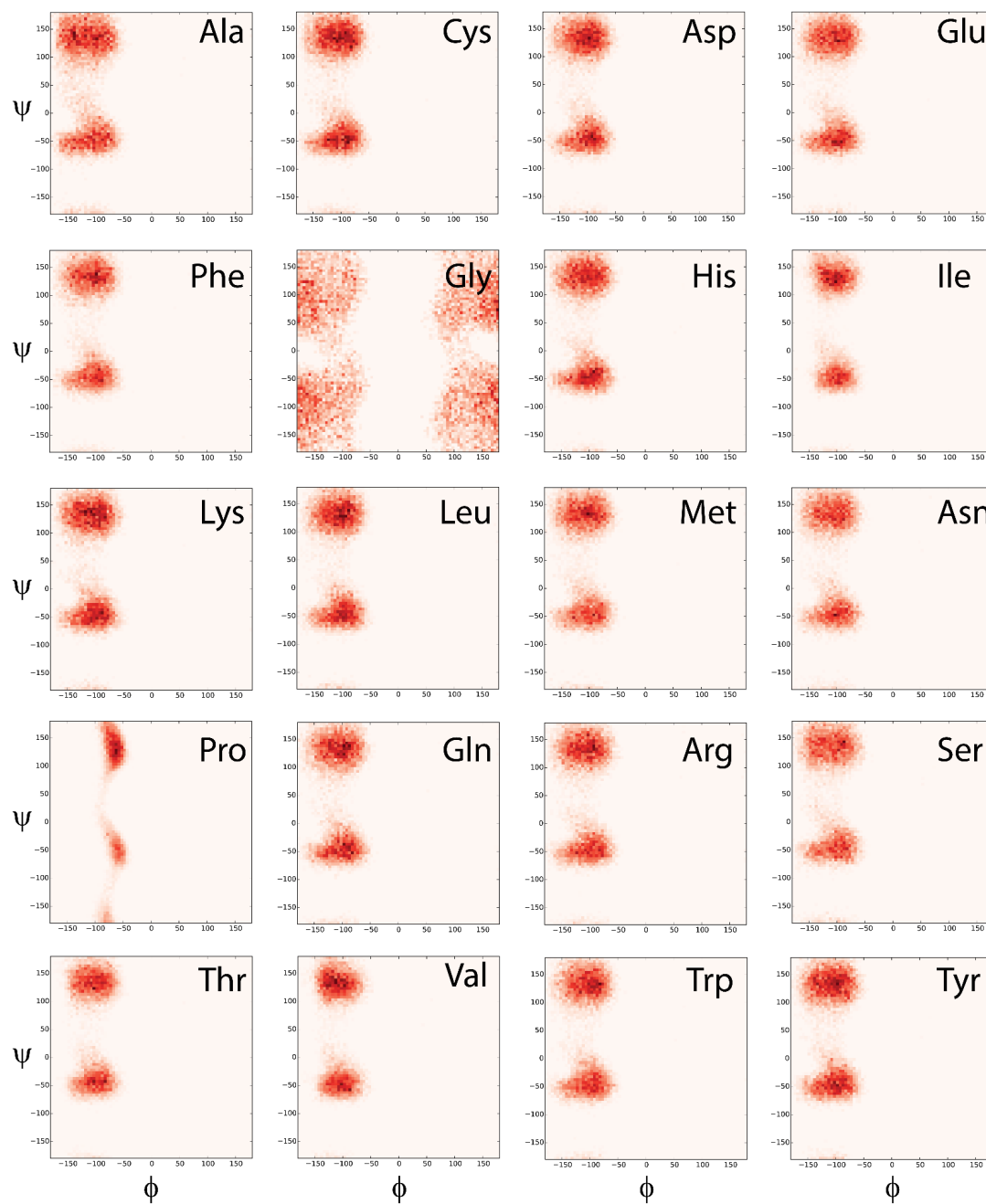
Fig. S1 Residue-specific Ramachandran maps used for FRC simulations. Ramachandran maps for all twenty amino acids performed as excluded volume simulations define the allowed isomeric states and are used by FRC simulations to construct the FRC ensembles.
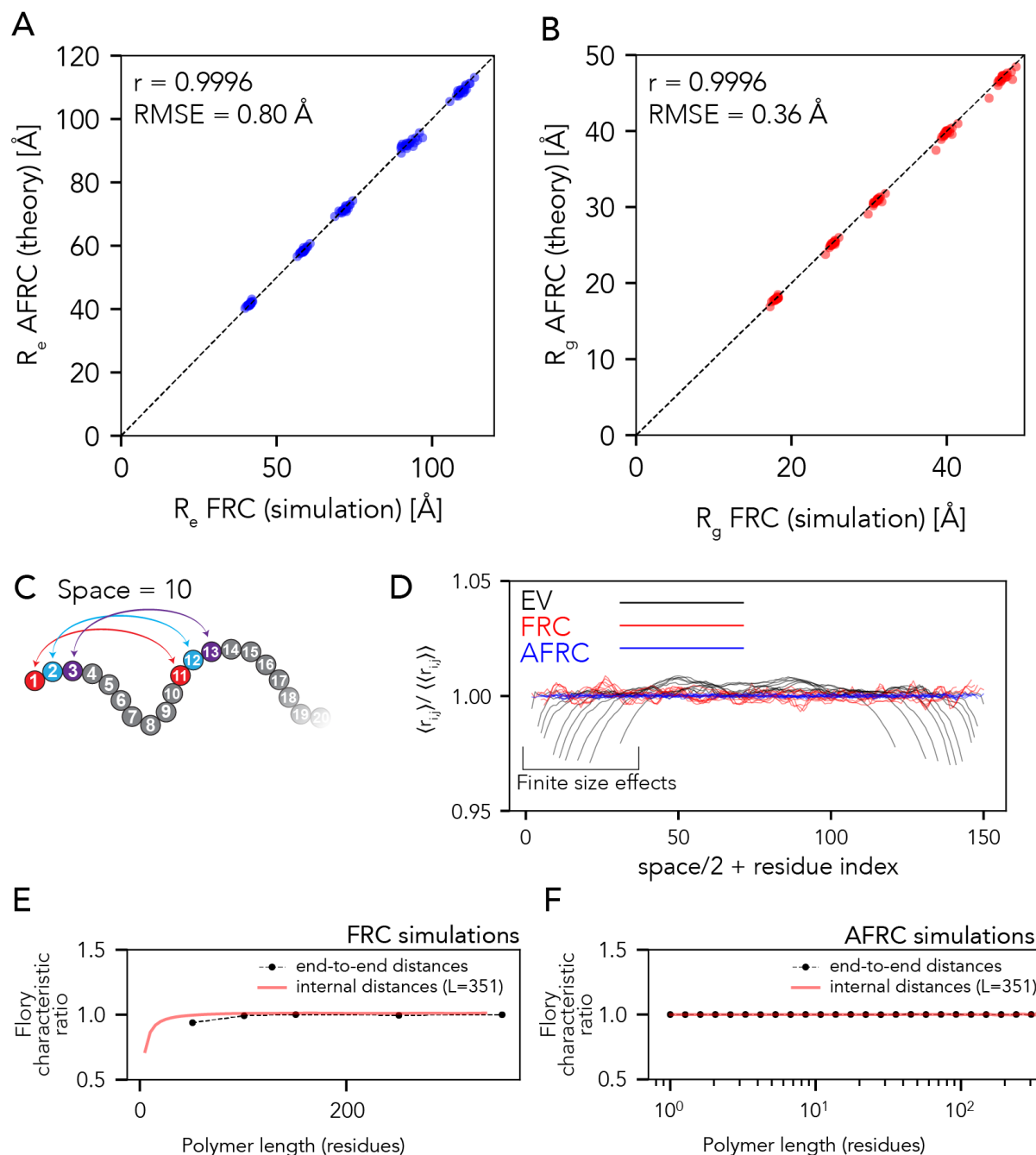
Fig. S2 Comparison between global dimensions from simulations vs. AFRC.
A. The correlation between the end-to-end distance (R_e) obtained from FRC simulations and AFRC analysis is shown. The comparisons here are for ensemble-average values for homopolymers derived from the twenty different amino acids for lengths of 51, 101, 151, 251, and 351 residues. **B.** The correlation between radius of gyration (R_g) values obtained from FRC simulations and AFRC analysis. Again, the comparisons here are for ensemble-average values

for homopolymers derived from the twenty different amino acids for lengths of 51, 101, 151, 251 and 351 residues. **C.** Schematic of the approach taken in panel D. **D.** For a 151-residue homopolymer, we calculated the average distance between all pairs of residues that are a fixed spacing apart for EV and FRC simulations and for the AFRC model. The inter-residue spacing used were 2, 6, 8, 10, 16, 20, 24, 32, 40, and 60 residues, and each spacing yields a different line. For example, for a spacing of 6 residues, we calculated the average distance between the following pairs of residues $\langle r_{1,7} \rangle$, $\langle r_{2,8} \rangle$, …, $\langle r_{145,151} \rangle$. Note the angle brackets here denote the ensemble-average distance. Each line represents the profile revealed by the set of inter-residue distances. For every point along the line, the y-axis position reports on the average distance normalized by the overall average distance for all residues of a given spacing. In contrast, the x-axis position is the location of the first residue of the two in a pair, to which half of the inter-residue spacing is added. For example, if we examined positions for $\langle r_{1,7} \rangle$, $\langle r_{2,8} \rangle$, …, $\langle r_{145,151} \rangle$ then the corresponding x-axis positions would be (1 + 0.5×6 = 4, 2 + 0.5×6 = 5, …, 145 + 0.5*×6 = 148). We take this approach such that the middle of the x-axis in the figure always corresponds to the central position in the polymer. For EV simulations, when one of the two residues in a pair falls near the end of the chain, we see a suppression of the inter-residue distances compared to the same inter-residue distance when both positions are internal to the chain. This is the expected result and reflects the fact that internal residues are 'repelled' by steric overlap with other residues, whereas end residues are less constrained. For FRC simulations and AFRC models, no such end effects are observed, reflecting the finite-size end effects do not influence ideal chains. **E**. We also calculated the Flory characteristic ratio (C_n) for chains of different lengths (black circles) and for intramolecular distances (red lines) for FRC simulations. The characteristic ratio enables correlations in chain dimensions to be assessed, and for FRC simulations, we see the expected deviation from 1 at shorter chain lengths (see supplemental methods). While these deviations are expected finite-size effects, their impact when comparing inter-residue distances is minimal (**Fig. 2**).
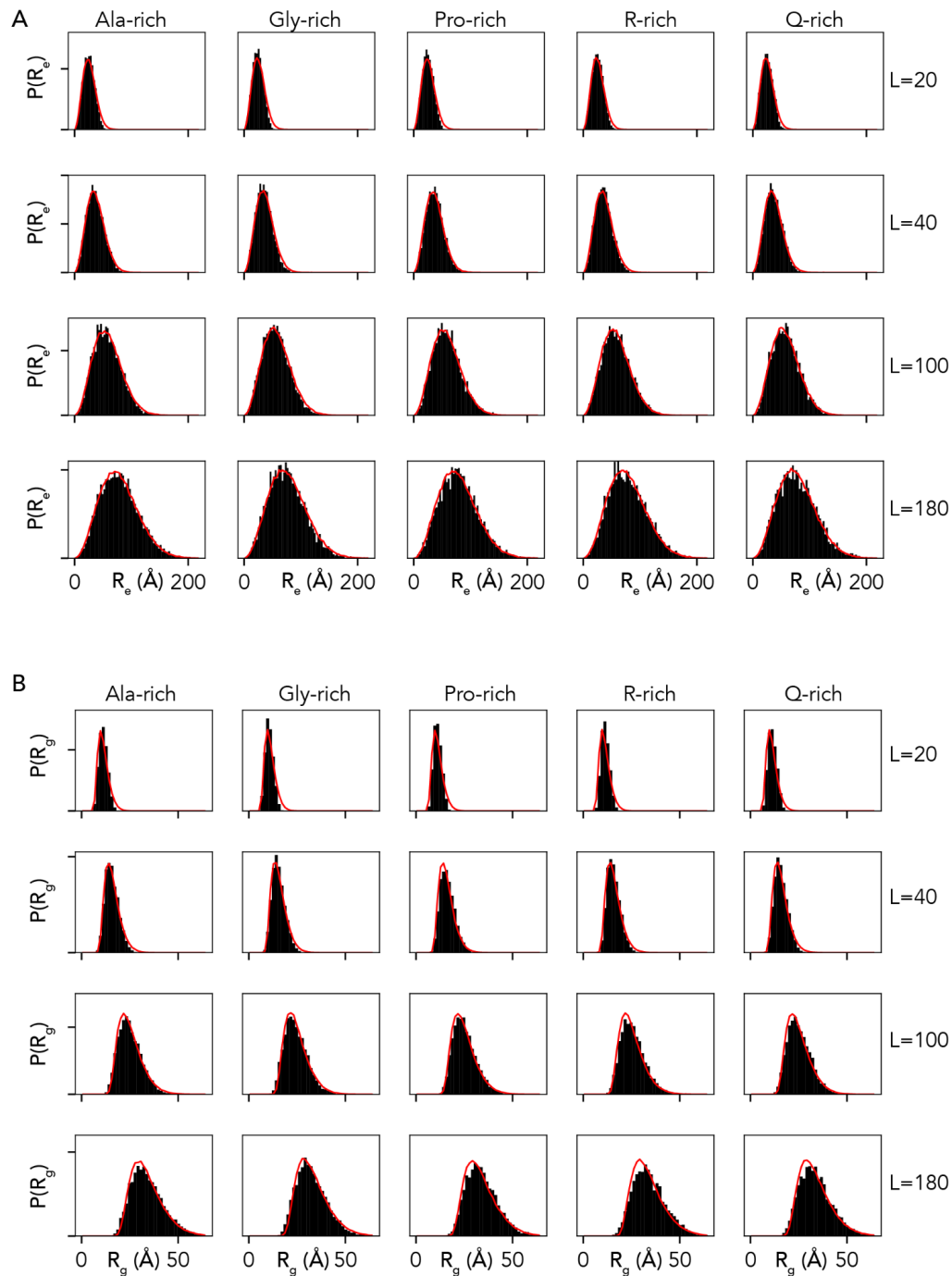
Fig. S3 Comparison of end-to-end distance distributions and radii of gyration distributions for select heteropolymers of variable composition and length. A. Comparison of end-to-end distance distributions. Empirical distributions obtained from simulations are shown in black, while predictions of the distribution from the AFRC are shown as red lines. **B.** Comparison of radii of gyration distributions. Empirical distributions obtained

from simulations shown in black, while predictions of the distribution from the AFRC are shown as red lines.
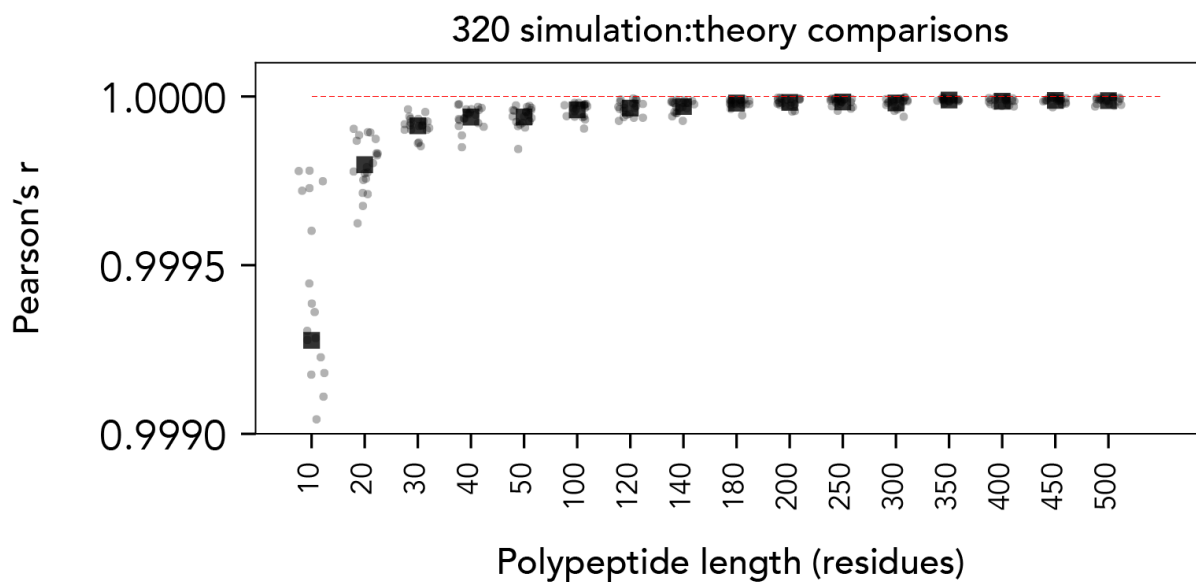
Fig. S4. Correlation between internal scaling profiles for random heteropolymers from FRC simulations vs. AFRC-derived internal scaling profiles. For each length (10,20,30, …, 500) 20 different heteropolymers, were generated where each heteropolymer is enriched (30%) in one of the twenty amino acids while the remaining residues are randomly selected. This yields 320 different internal scaling comparisons (16 lengths with 20 amino acids).
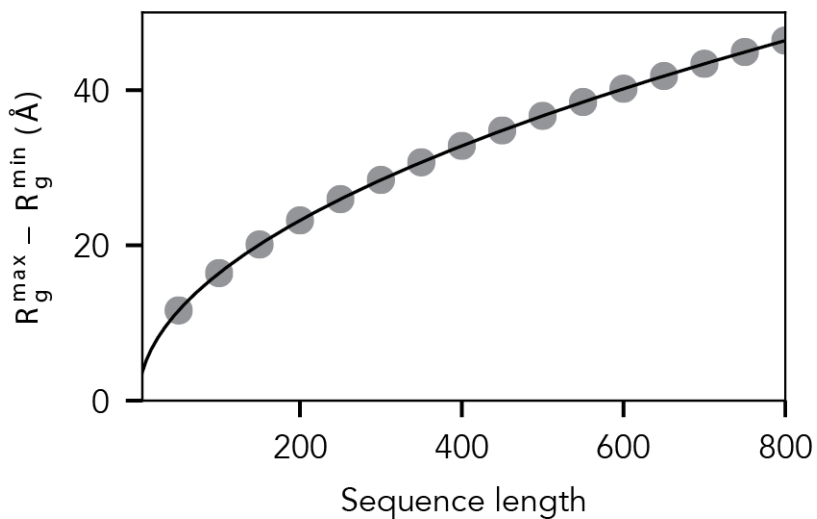
Fig. S5. Difference in radii of gyration based on empirical min and max values reveals the length-dependent variation in expected accessible radii of gyration values.
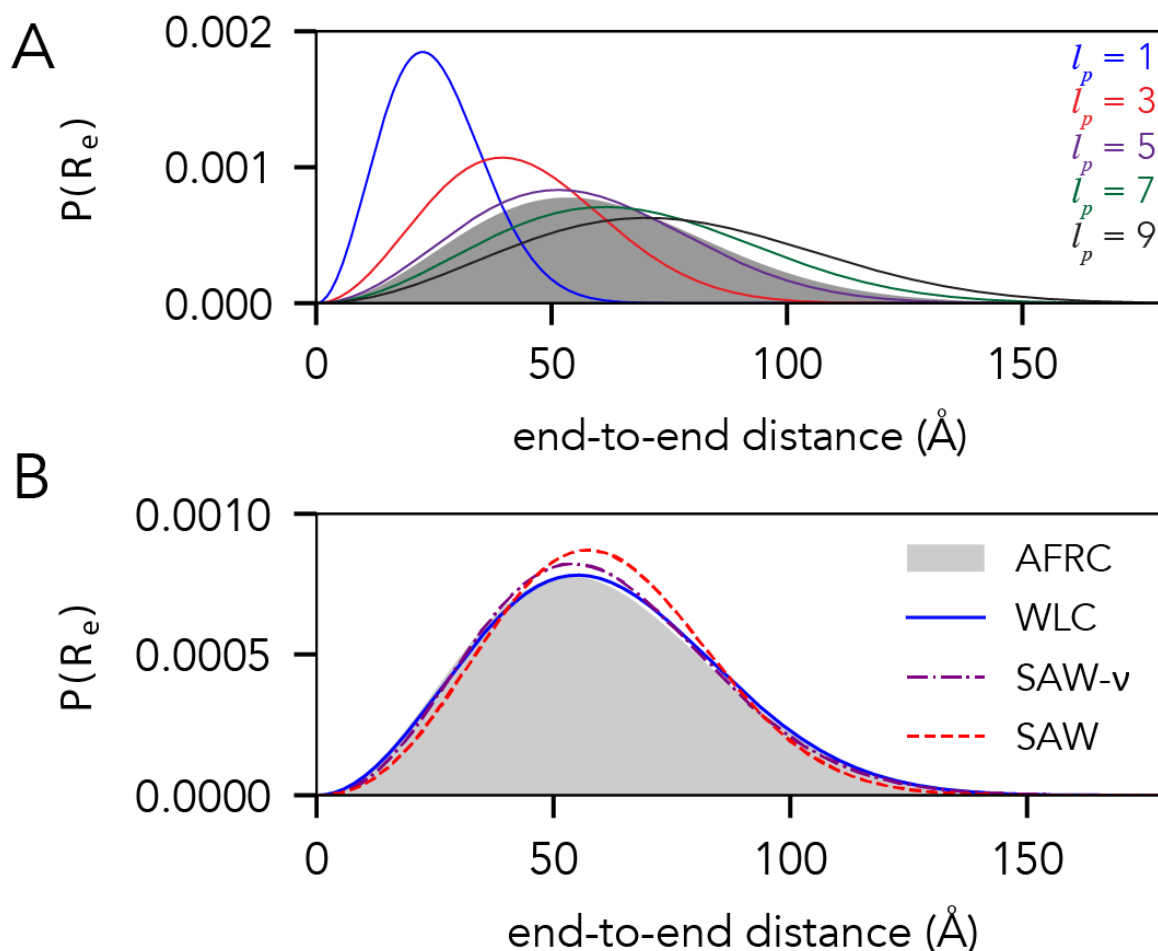
Fig. S6. Comparison of the end-to-end distance distributions for the AFRC with existing polymer models. **A.** Comparison of the AFRC model (grey shaded area) for 100-residue polyalanine chain (A_{100}) with Worm-Like chain (WLC)-derived distributions, where the WLC monomer size is fixed at 3.8 Å, and the persistence length varies from 1 Å to 9 Å. **B.** Comparison of AFRC, WLC, SAW-v, and SAW models in which model input parameters were selected to reproduce the AFRC end-to-end distance distribution for an A_{100} chain. The WLC model uses an amino acid size of 3.8 Å and a persistence length of 5.7 Å. The SAW-v model uses a prefactor of 5.8 Å and a v of 0.5. The SAW model uses a prefactor of 4.1 Å.
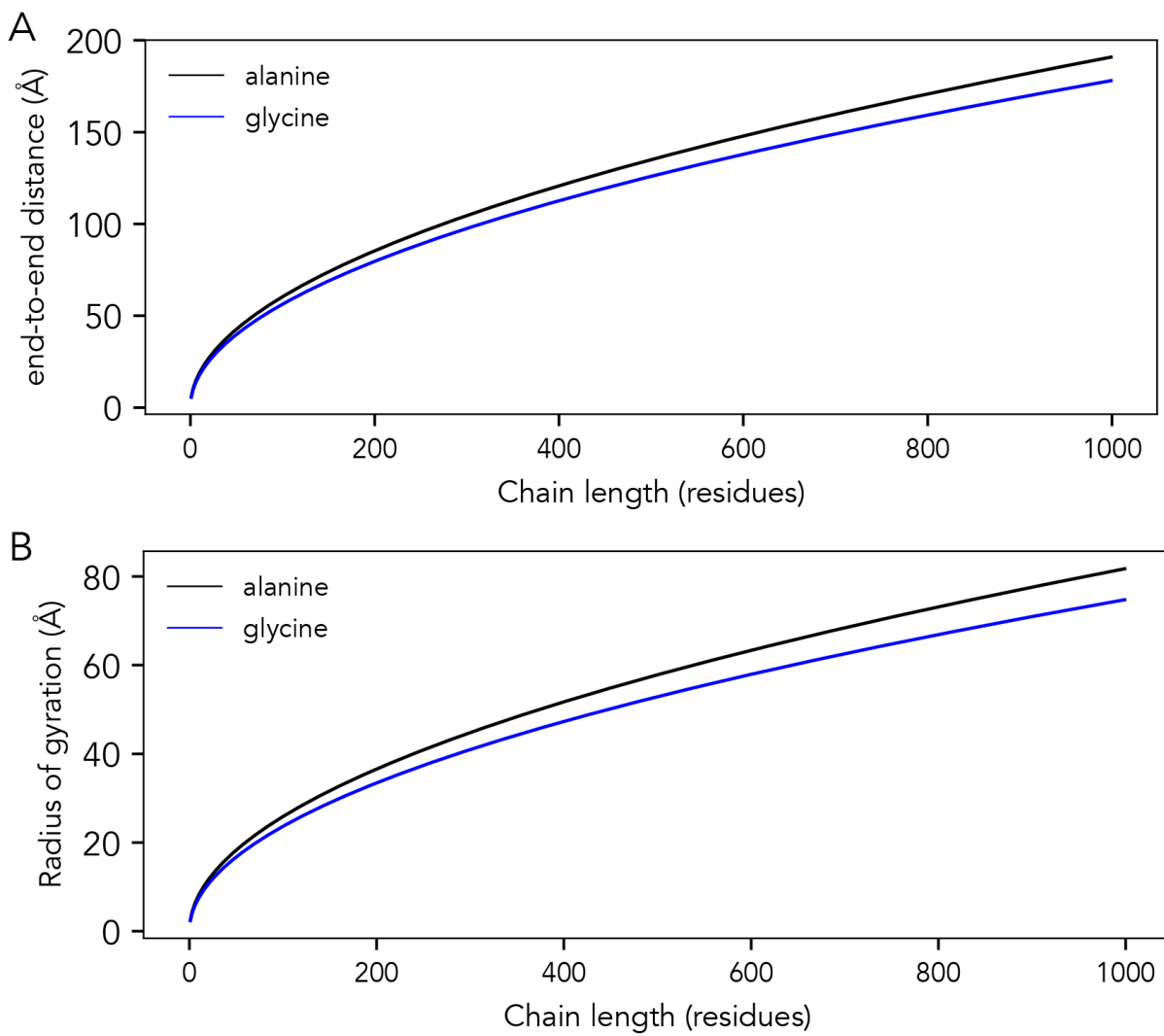
Fig. S7. Comparison of chain dimensions obtained from the AFRC model for poly-alanine vs. poly-glycine, examining end-to-end distance (**A**) and radius of gyration (**B**).

3. SUPPLEMENTARY TABLES

Amino acid	R_{ij} RMS (Å)	R_{ij} (Å)	X_0 (Å^{-1})
A	6.5463	6.0381	0.5405
C	6.2676	5.7826	0.5635
D	6.3994	5.911	0.5567
E	6.2649	5.768	0.5613
F	6.2519	5.7612	0.5571
G	6.1045	5.6324	0.5911
H	6.2156	5.7262	0.5645
I	6.4353	5.9361	0.5483
K	6.306	5.8272	0.5533
L	6.2636	5.7801	0.5605
M	6.3813	5.8894	0.5501
N	6.2652	5.773	0.5598
P	6.4323	5.9388	0.5599
Q	6.2547	5.7719	0.5617
R	6.279	5.7921	0.5531
S	6.3161	5.8364	0.5553
T	6.1995	5.7242	0.5695
V	6.3204	5.8409	0.5571
W	6.3	5.814	0.5539
Y	6.3188	5.8266	0.5543

Table S1 Model parameters obtained by fitting against FRC simulations.

Name	Sequence
Ash1	GASASSSPSP STPTKSGKMR SRSSSPVRPK AYTPSPRSPN YHRFALDSPP QSPRRSSNSS ITKKGSRRSS GSSPTRHTTR VCV
p53	MEEPQSDPSV EPPLSQETFS DLWKLLPENN VLSPLPSQAM DDLMLSPDDI EQWFTEDPGP DEAPRMPEAA PPVAPAPAAP TPAAPAPAPS W
p27	GSHMKGACKV PAQESQDVSG SRPAAPLIGA PANSEDTHLV DPKTDPSDSQ TGLAEQCAGI RKRPATDDSS TQNKRANRTE ENVSDGSPNA GSVEQTPKKP GLRRQT
Notch	MARKRRRQHG QLWFPEGFKV SEASKKKRRE PLGEDSVGLK PLKNASDGAL MDDNQNEWGD EDLETKKFRF EEPVVLPDLD DQTDHRQWTQ QHLDAADLRM SAMAPTPPQG EVDADCMDVN VRGPDGFTPL LE
ACTR	GTQNRPLLRN SLDDLVGPPS NLEGQSDERA LLDQLHTLLS NTDATGLEEI DRALGIPELV NQGQALEPKQ D
drkN	MEAIAKHDFS ATADDELSFR KTQILKILNM EDDSNWYRAE LDGKEGLIPS NYIEMKNHD
Ntail	MHHHHHHTTE DKISRAVGPR QAQVSFLHGD QSENELPRLG GKEDRRVKQS RGEARESYRE TGPSRASDAR AAHLPTGTPL DIDTASESSQ DPQDSRRSAD ALLRLQAMAG ISEEQGSDTD TPIVYNDRNL LD
asyn	MDVFMKGLSK AKEGVVAAAE KTKQGVAEAA GKTKEGVLYV GSKTKEGVVH GVATVAEKTK EQVTNVGGAV VTGVTAVAQK TVEGAGSIAA ATGFVKKDQL GKNEEGAPQE GILEDMPVDP DNEAYEMPSE EGYQDYEPEA
A1-LCD	GSMASASSSQ RGRSGSGNFG GGRGGGFGGN DNFGRGGNFS GRGGFGGSRG GGGYGGSGDG YNGFGNDGSN FGGGGSYNDF GNYNNQSSNF GPMKGGNFGG RSSGPYGGGG QYFAKPRNQG GYGGSSSSSS YGSGRRF

Table S2. Sequences from simulations. Full sequences used from all-atom simulations. Amino acids are colored by chemical type as per localCIDER[10].

Name	N	R_g (Å)	R_g/R_g^{θ}	R_e (Å)	R_e/R_e^{θ}	ν^{app} [a]	Quality of ν^{app} fit [b]
Ash1	83	28.9	1.27	68.95	1.30	0.61	GOOD
p53	91	29.4	1.23	77.73	1.39	0.66	GOOD
p27	107	28.3	1.09	59.15	0.98	0.49	POOR
Notch	132	29.3	1.02	52.16	0.78	0.34	POOR
ACTR	71	21.1	1.01	41.45	0.85	0.50	GOOD
drkN	59	19.3	1.00	45.26	1.01	0.43	GOOD
Ntail	132	26.3	0.92	58.11	0.87	0.39	POOR
asyn	140	25.6	0.87	46.47	0.67	0.23	POOR
A1-LCD	137	24.1	0.84	54.37	0.81	0.47	GOOD

[a] Estimated ν^{app} based on linear fitting of the internal scaling regime using SOURSOP.
[b] Quality of fit based on the reduced chi-squared from the fit.

Table S3: Simulation and AFRC-derived parameters for all-atom simulations.

Table S4: SAXS sequences and values (note table caption comes before table as table is 36 pages long). Note that when error is reported as 0, this means an accurate error could not be determined, not that the measurement is perfect.

Protein name	R_g (Å)	R_g error (Å)	Amino acid sequence	Reference
Nucleoporin Nup49 (N49)	15.9	1.3	GCQTSRGLFGNNNTNNINNSSSGMNNASAGLF GSKPCA	Fuertes, et al. PNAS (2017) 114, E6342–E6351.
Heh2 (NLS)	24	3	ACETNKRKREQISTDNEAKMQIQEEKSPKKKRK KRSSKANKPPECA	Fuertes, et al. PNAS (2017) 114, E6342–E6351.
VSV Protein Phosphoprotein P	24	1	HHHHHELMDNLTKVREYLKSYSRLDQAVGEIDEI EAQRAEKSNYELFQEDGVEEHTKPSYFQAADDS	Leyrat, C., Jensen, M.R., Ribeiro, E.A., Gérard, F.C.A., Ruigrok, R.W.H., Blackledge, M., and Jamin, M. (2011). The N0-binding region of the vesicular stomatitis virus phosphoprotein is globally disordered but contains transient α-helices. Protein Sci. 20, 542–556.
LS	27.9	1	SPPGKPQGPPQQEGNKPQGPPPPGKPQGPPPA GGNPQQPQAPPAGKPQGPPPPPQGGRPPRPA QGQQPPQ	Boze, H., Marlin, T., Durand, D., Pérez, J., Vernhet, A., Canon, F., Sarni-Manchado, P., Cheynier, V., and Cabane, B. (2010). Proline-rich salivary proteins have extended conformations. Biophys. J. 99, 656–665.
Nup153_NUS	24.9	1.3	GCPSASPAFGANQTPTFGQSQGASQPNPPGFG SISSSTALFPTGSQPAPPTFGTVSSSSQPPVFGQ QPSQSAFGSGTTPNCA	Fuertes, et al. PNAS (2017) 114, E6342–E6351.

Sic1	30	4	GSMTPSTPPRSRGTRYLAQPSGNTSSSALMQG QKTPQKPSQNLVPVTPSTTKSFKNAPLLAPPNSN MGMTSPFNGLTSPQRSPFPKSSVKRT	Gomes G-NW, Krzeminski M, Namini A, Martin EW, Mittag T, Head-Gordon T, et al. Conformational Ensembles of an Intrinsically Disordered Protein Consistent with NMR, SAXS, and Single-Molecule FRET. J Am Chem Soc. 2020;142: 15697–15710.
chloroplastic calvin cycle protein	23		HHHHHHHHHHHSSGHIEGRHMSGQPAVDLNKKV QDAVKEAEDACAKGTSADCAVAWDTVEELSAAV SHKKDAVKADVTLTDPLEAFCKDAPDADECRVY ED	Launay H, Barré P, Puppo C, Zhang Y, Maneville S, Gontero B, Receveur-Bréchot V, J Mol Biol 430(8):1218-1234 (2018)
Antitermination protein N (from lambda phage)	38	3.5	MDAQTRRRERRAEKQAQWKAANPLLVGVSAKP VNRPILSLNRKPKSRVESALNPIDLTVLAEYHKQI ESNLQRIERKNQRTWYSKPGERGITCSGRQKIK GKSIPLI	Johansen, D., Trewhella, J., and Goldenberg, D.P. (2011). Fractal dimension of an intrinsically disordered protein: small-angle X-ray scattering and computational study of the bacteriophage λ N protein. Protein Sci. 20, 1955–1970.
Nup153_NUL	30	3	GCGFKGFDTSSSSSNSAASSSFKFGVSSSSSGP SQTLTSTGNFKFGDQGGFKIGVSSDSGSINPMS EGFKFSKPIGDFKFGVSSESKPEEVKKDSKNDNF KFGLSSGLSNPVCA	Fuertes, et al. PNAS (2017) 114, E6342–E6351.
DARPP-32 (aka Protein phosphatase 1 regulatory subunit 1B)	28.28		MDPKDRKKIQFSVPAPPSQLDPRQVEMIRRRRP TPALLFRVSEHSSPEEESSPHQRTSGEGHHPKS KRPNPCAYTPPSLKAVQRIAESHLQTISNLSENQ ASEEEDELGELRELGYPQ	Marsh, J.A., Dancheck, B., Ragusa, M.J., Allaire, M., Forman-Kay, J.D., and Peti, W. (2010). Structural diversity in free and bound states of intrinsically disordered protein phosphatase 1 regulators. Structure 18, 1094–1103.

Il-1	41		GKPVGRRPQGGNQPQRPPPPPGKPQGPPPQG GNQSQGPPPPPGKPEGRPPQGRNQSQGPPPH PGKPERPPPQGGNQSQGTPPPPGKPERPPPQG GNQSHRPPPPPGKPERPPPQGGNQSRGPPPH RGKPEGPPPQEGNKSR	Boze, H., Marlin, T., Durand, D., Pérez, J., Vernhet, A., Canon, F., Sarni-Manchado, P., Cheynier, V., and Cabane, B. (2010). Proline-rich salivary proteins have extended conformations. Biophys. J. 99, 656–665.
Fhua	33.4		ESAWGPAATIAARQSATGTKTDTPIQKVPQSISV VTAEEMALHQPKSVKEALSYTPGVSVGTRGASN TYDHLIIRGFAAEGQSQNNYLNGLKLQGNFYNDA VIDPYMLERAEIMRGPVSVLYGKSSPGGLLNMVS KRPTTEP	Riback, J.A., Bowman, M.A., Zmyslowski, A.M., Knoverek, C.R., Jumper, J.M., Hinshaw, J.R., Kaye, E.B., Freed, K.F., Clark, P.L., and Sosnick, T.R. (2017). Innovative scattering analysis shows that hydrophobic disordered proteins are expanded in water. Science 358, 238–241.
N98	28.6	1.3	GCFNKSFGTPFGGGTGGFGTTSTFGQNTGFGT TSGGAFGTSAFGSSNNTGGLFGNSQTKPGGLF GTSSFSQPATSTSTGFGFGTSTGTANTLFGTAST GTSLFSSQNNAFAQNKPTGFGNFGTSTSSGGLF GTTNTTSNPFGSTSGSLFGPCA	Fuertes, et al. PNAS (2017) 114, E6342–E6351.
Protein Phosphatase Inhibitor 2	34.6		PIKGILKNKTSTTSSMVASAEQPRGNVDEELSKK SQKWDEMNILATYHPADKDYGLMKIDEPSTPYH SMMGDDEDACSDTEATEAMAPDILARKLAAAEG LEPKYRIQEQESSGEEDSDLSPEEREKKRQFEM KRKLHYNEGLNIKLARQLISKDL	Marsh, J.A., Dancheck, B., Ragusa, M.J., Allaire, M., Forman-Kay, J.D., and Peti, W. (2010). Structural diversity in free and bound states of intrinsically disordered protein phosphatase 1 regulators. Structure 18, 1094–1103.
Nsp1	41	3	GCNFNTPQQNKTPFSFGTANNNSNTTNQNSST GAGAFGTGQSTFGFNNSAPNNTNNANSSITPAF GSNNTGNTAFGNSNPTSNVFGSNNSTTNTFGSN SAGTSLFGSSSAQQTKSNGTAGGNTFGSSSLFN	Fuertes, et al. PNAS (2017) 114, E6342–E6351.

			NSTNSNTTKPAFGGLNFGGGNNTTPSSTGNANT SNNLFGATANANCA	
IBB	32	2	GCTNENANTPAARLHRFKNKGKDSTEMRRRRIE VNVELRKAKKDDQMLKRRNVSSFPDDATSPLQE NRNNQGTVNWSVDDIVKGINSSNVENQLQATCA	Fuertes, et al. PNAS (2017) 114, E6342–E6351.
Ash1	28.5	3.4	GASASSSPSPSTPTKSGKMRSRSSSPVRPKAYT PSPRSPNYHRFALDSPPQSPRRSSNSSITKKGS RRSSGSSPTRHTTRVCV	Martin, E.W., Holehouse, A.S., Grace, C.R., Hughes, A., Pappu, R.V., and Mittag, T. (2016). Sequence Determinants of the Conformational Properties of an Intrinsically Disordered Protein Prior to and upon Multisite Phosphorylation. J. Am. Chem. Soc. 138, 15323–15335.
pAsh1	27.5	1.2	GASASSSPSPSTPTKSGKMRSRSSSPVRPKAYT PSPRSPNYHRFALDSPPQSPRRSSNSSITKKGS RRSSGSSPTRHTTRVCV	Martin, E.W., Holehouse, A.S., Grace, C.R., Hughes, A., Pappu, R.V., and Mittag, T. (2016). Sequence Determinants of the Conformational Properties of an Intrinsically Disordered Protein Prior to and upon Multisite Phosphorylation. J. Am. Chem. Soc. 138, 15323–15335.
PIR domain (GRB14)	27		YGMQLYQNYMHPYQGRSGCSSQSISPMRSISE NSLVAMDFSGQKSRVIENPTEALSVAVEEGLAW RKKGCLRLGTHGSPTASSQSSATNMAIHRSQPW	Moncoq, K., Broutin, I., Craescu, C.T., Vachette, P., Ducruix, A., and Durand, D. (2004). SAXS study of the PIR domain from the Grb14 molecular adaptor: a natively unfolded protein with a transient structure primer? Biophys. J. 87, 4056–4064.

RpII215_gibbs	28	0.7	YSPGNAYSPSSSNYSPNSPSYSPTSPSYSPSSP SYSPTSPCYSPTSPSYSPTSPNYTPVTPSYSPTS PNYSASPQ	Gibbs, E.B., Lu, F., Portz, B., Fisher, M.J., Medellin, B.P., Laremore, T.N., Zhang, Y.J., Gilmour, D.S., and Showalter, S.A. (2017). Phosphorylation induces sequence-specific conformational switches in the RNA polymerase II C-terminal domain. Nat. Commun. 8, 15233.
RpII215_portz	51.8		SPSYSPTSPNYTASSPGGASPNYSPSSPNYSPT SPLYASPRYASTTPNFNPQSTGYSPSSSGYSPT SPVYSPTVQFQSSPSFAGSGSNIYSPGNAYSPS SSNYSPNSPSYSPTSPSYSPSSPSYSPTSPCYS PTSPSYSPTSPNYTPVTPSYSPTSPNYSASPQYS PASPAYSQTGVKYSPTSPTYSPPSPSYDGSPGS PQYTPGSPQYSPASPKYSPTSPLYSPSSPQHSP SNQYSPTGSTYSATSPRYSPNMSIYSPSSTKYSP TSPTYTPTARNYSPTSPMYSPTAPSHYSPTSPAY SPSSPTFEESED	Portz, B., Lu, F., Gibbs, E.B., Mayfield, J.E., Rachel Mehaffey, M., Zhang, Y.J., Brodbelt, J.S., Showalter, S.A., and Gilmour, D.S. (2017). Structural heterogeneity in the intrinsically disordered RNA polymerase II C-terminal domain. Nat. Commun. 8, 15231.
ACTR	25		GPSGTQNRPLLRNSLDDLVGPPSNLEGQSDERA LLDQLHTLLSNTDATGLEEIDRALGIPELVNQGQA LEPKQDSGGPR	Borgia, A., Zheng, W., Buholzer, K., Borgia, M.B., Schüler, A., Hofmann, H., Soranno, A., Nettels, D., Gast, K., Grishaev, A., et al. (2016). Consistent View of Polypeptide Chain Expansion in Chemical Denaturants from Multiple Experimental Methods. J. Am. Chem. Soc. 138, 11714–11726.
Msh6	56	2	MAPATPKTSKTAHFENGSTSSQKKMKQSSLLSF FSKQVPSGTPSKKVQKPTPATLENTATDKITKNP QGGKTGKLFVDVDEDNDLTIAEETVSTVRSDIMH SQEPQSDTMLNSNTTEPKSTTTDEDLSSSQSRR NHKRRVNYAESDDDDSDTTFTAKRKKGKVVDSE SDEDEYLPDKNDGDEDDDIADDKEDIKGELAEDS GDDDDLISLAETTSKKKFSYNTSHSSSPFTRNISR DNSKKKSRPNQAPSRSYNPSHSQPSATSKSSKF	Shell, S.S., Putnam, C.D., and Kolodner, R.D. (2007). The N terminus of Saccharomyces cerevisiae Msh6 is an unstructured tether to PCNA. Mol. Cell 26, 565–578.

			NKQNEERYQWLVDERDAQRRPKSDPEYDPRTL YIP	
AN16	50	2	AQTPSSQYGAPAQTPSSQYGAPAQTPSSQYGA PAQTPSSQYGAPAQTPSSQYGAPAQTPSSQYG APAQTPSSQYGAPAQTPSSQYGAPAQTPSSQY GAPAQTPSSQYGAPAQTPSSQYGAPAQTPSSQ YGAPAQTPSSQYGAPAQTPSSQYGAPAQTPSS QYGAPAQTPSSQYGAP	Nairn, K.M., Lyons, R.E., Mulder, R.J., Mudie, S.T., Cookson, D.J., Lesieur, E., Kim, M., Lau, D., Scholes, F.H., and Elvin, C.M. (2008). A synthetic resilin is largely unstructured. Biophys. J. 95, 3358–3365.
HrpO	35		MEDTLEDDPQRAALEQVISLLTPVRQHRQASAE RAHRHAQVELKSMLDHLSKIRASLDQERDNHKR RREGLSQEHLEKTISPNDIDRWHEKEKHMLDRL ACIRQDVQQQQLRVAEQQALLEQKRLQAKASQR AVEKLACMEETLNEEG	Gazi, A.D., Bastaki, M., Charova, S.N., Gkougkoulia, E.A., Kapellios, E.A., Panopoulos, N.J., and Kokkinidis, M. (2008). Evidence for a Coiled-coil Interaction Mode of Disordered Proteins from Bacterial Type III Secretion Systems. J. Biol. Chem. 283, 34062–34068.
alpha-syn	41	1	MDVFMKGLSKAKEGVVAAAEKTKQGVAEAAGK TKEGVLYVGSKTKEGVVHGVATVAEKTKEQVTN VGGAVVTGVTAVAQKTVEGAGSIAAATGFVKKD QLGKNEEGAPQEGILEDMPVDPDNEAYEMPSEE GYQDYEPEA	Uversky, V.N., Li, J., Souillac, P., Millett, I.S., Doniach, S., Jakes, R., Goedert, M., and Fink, A.L. (2002). Biophysical properties of the synucleins and their propensities to fibrillate: inhibition of alpha-synuclein assembly by beta- and gamma-synucleins. J. Biol. Chem. 277, 11970–11978.
NTail	27.2	0.5	TTEDKISRAVGPRQAQVSFLHGDQSENELPRLG GKEDRRVKQSRGEARESYRETGPSRASDARAA HLPTGTPLDIDTASESSQDPQDSRRSADALLRLQ AMAGISEEQGSDTDTPIVYNDRNLLD	Longhi, S., Receveur-Bréchot, V., Karlin, D., Johansson, K., Darbon, H., Bhella, D., Yeo, R., Finet, S., and Canard, B. (2003). The C-terminal domain of the measles virus nucleoprotein is intrinsically disordered and folds upon

				binding to the C-terminal moiety of the phosphoprotein. J. Biol. Chem. 278, 18638–18648.
ERM	39.6	0.7	MDGFYDQQVPFMVPGKSRSEECRGRPVIDRKR KFLDTDLAHDSEELFQDLSQLQEAWLAEAQVPD DEQFVPDFQSDNLVLHAPPPTKIKRELHSPSSEL SSCSHEQALGANYGEKCLYNYCA	Lens, Z., Dewitte, F., Monté, D., Baert, J.-L., Bompard, C., Sénéchal, M., Van Lint, C., de Launoit, Y., Villeret, V., and Verger, A. (2010). Solution structure of the N-terminal transactivation domain of ERM modified by SUMO-1. Biochem. Biophys. Res. Commun. 399, 104–110.
Neuroligin-3	33	3	YRKDKRRQEPLRQPSPQRGAGAPELGAAPEEE LAALQLGPTHHECEAGPPHDTLRLTALPDYTLTL RRSPDDIPLMTPNTITMIPNSLVGLQTLHPYNTFA AGFNSTGLPHSHSTTRV	Paz, A., Zeev-Ben-Mordehai, T., Lundqvist, M., Sherman, E., Mylonas, E., Weiner, L., Haran, G., Svergun, D.I., Mulder, F.A.A., Sussman, J.L., et al. (2008). Biophysical characterization of the unstructured cytoplasmic domain of the human neuronal adhesion protein neuroligin 3. Biophys. J. 95, 1928–1944.
Prothymosin alpha	37.8	0.9	MSDAAVDTSSEITTKDLKEKKEVVEEAENGRDAP ANGNAENEENGEQEADNEVDEEEEEGGEEEEE EEEGDGEEEDGDEDEEAESATGKRAAEDDEDD DVDTKKQKTDEDD	Uversky, V.N., Gillespie, J.R., Millett, I.S., Khodyakova, A.V., Vasiliev, A.M., Chernovskaya, T.V., Vasilenko, R.N., Kozlovskaya, G.D., Dolgikh, D.A., Fink, A.L., et al. (1999). Natively Unfolded Human Prothymosin α Adopts Partially Folded Collapsed Conformation at Acidic pH. Biochemistry 38, 15009–15016.
Fez1	36	1	QIQEEEETLQDEEVWDALTDNYIPSLSEDWRDP NIEALNGNCSDTEIHEKEEEEFNEKSENDSGINE	Alborghetti, M.R., Furlan, A.S., Silva, J.C., Paes Leme, A.F.,

			EPLLTADQVIEEIEEMMQNSPDPEEEEEVLEEED GG	Torriani, I.C.L., and Kobarg, J. (2010). Human FEZ1 Protein Forms a Disulfide Bond Mediated Dimer: Implications for Cargo Transport. J. Proteome Res. 9, 4595–4603.
HIV-TAT	33	1.05	MEPVDPRLEPWKHPGSQPRTACTNCYCKKCCF HCQVCFIRKALGISYGRKKRRQRRRAPQDSETH QVSPPKQPASQPRGDPTGPKESKKKVERETETH PVN	Foucault, M., Mayol, K., Receveur-Bréchot, V., Bussat, M.-C., Klinguer-Hamour, C., Verrier, B., Beck, A., Haser, R., Gouet, P., and Guillon, C. (2010). UV and X-ray structural studies of a 101-residue long Tat protein from a HIV-1 primary isolate and of its mutated, detoxified, vaccine candidate. Proteins 78, 1441–1456.
p531-91	28.7	0.3	MEEPQSDPSVEPPLSQETFSDLWKLLPENNVLS PLPSQAMDDLMLSPDDIEQWFTEDPGPDEAPR MPEAAPPVAPAPAAPTPAAPAPAPSW	Wells, M., Tidow, H., Rutherford, T.J., Markwick, P., Jensen, M.R., Mylonas, E., Svergun, D.I., Blackledge, M., and Fersht, A.R. (2008). Structure of tumor suppressor p53 and its intrinsically disordered N-terminal transactivation domain. Proc. Natl. Acad. Sci. U. S. A. 105, 5762–5767.
Tau - ht40	65	3	MAEPRQEFEVMEDHAGTYGLGDRKDQGGYTM HQDQEGDTDAGLKESPLQTPTEDGSEEPGSETS DAKSTPTAEDVTAPLVDEGAPGKQAAAQPHTEIP EGTTAEEAGIGDTPSLEDEAAGHVTQARMVSKS KDGTGSDDKKAKGADGKTKIATPRGAAPPGQKG QANATRIPAKTPPAPKTPPSSGEPPKSGDRSGY SSPGSPGTPGSRSRTPSLPTPPTREPKKVAVVR TPPKSPSSAKSRLQTAPVPMPDLKNVKSKIGSTE NLKHQPGGGKVQIINKKLDLSNVQSKCGSKDNIK HVPGGGSVQIVYKPVDLSKVTSKCGSLGNIHHKP	E. Mylonas, A. Hascher, P. Bernado´, M. Blackledge, E. Mandelkow and D. I. Svergun, Biochemistry, 2008, 47, 10345–10353.

			GGGQVEVKSEKLDFKDRVQSKIGSLDNITHVPG GGNKKIETHKLTFRENAKAKTDHGAEIVYKSPVV SGDTSPRHLSNVSSTGSIDMVDSPQLATLADEV SASLAKQGL	
Tau - K32	42	3	SSPGSPGTPGSRSRTPSLPTPPTREPKKVAVVR TPPKSPSSAKSRLQTAPVPMPDLKNVKSKIGSTE NLKHQPGGGGKVQIINKKLDLSNVQSKCGSKDNIK HVPGGGSVQIVYKPVDLSKVTSKCGSLGNIHHKP GGGGQVEVKSEKLDFKDRVQSKIGSLDNITHVPG GGNKKIETHKLTFRENAKAKTDHGAEIVY	E. Mylonas, A. Hascher, P. Bernado´, M. Blackledge, E. Mandelkow and D. I. Svergun, Biochemistry, 2008, 47, 10345– 10353.
Tau - K16	39	3	SSPGSPGTPGSRSRTPSLPTPPTREPKKVAVVR TPPKSPSSAKSRLQTAPVPMPDLKNVKSKIGSTE NLKHQPGGGGKVQIINKKLDLSNVQSKCGSKDNIK HVPGGGSVQIVYKPVDLSKVTSKCGSLGNIHHKP GGGGQVEVKSEKLDFKDRVQSKIGSLDNITHVPG GGNKKIE	E. Mylonas, A. Hascher, P. Bernado´, M. Blackledge, E. Mandelkow and D. I. Svergun, Biochemistry, 2008, 47, 10345– 10353.
Tau - K18	38	3	QTAPVPMPDLKNVKSKIGSTENLKHQPGGGGKVQ IINKKLDLSNVQSKCGSKDNIKHVPGGGSVQIVYK PVDLSKVTSKCGSLGNIHHKPGGGGQVEVKSEKL DFKDRVQSKIGSLDNITHVPGGGNKKIE	E. Mylonas, A. Hascher, P. Bernado´, M. Blackledge, E. Mandelkow and D. I. Svergun, Biochemistry, 2008, 47, 10345– 10353.
Tau - ht23	53	3	MAEPRQEFEVMEDHAGTYGLGDRKDQGGYTM HQDQEGDTDAGLKAEEAGIGDTPSLEDEAAGHV TQARMVSKSKDGTGSDDKKAKGADGKTKIATPR GAAPPGQKGQANATRIPAKTPPAPKTPPSSGEP PKSGDRSGYSSPGSPGTPGSRSRTPSLPTPPTR EPKKVAVVRTPPKSPSSAKSRLQTAPVPMPDLK NVKSKIGSTENLKHQPGGGKVQIVYKPVDLSKVT SKCGSLGNIHHKPGGGQVEVKSEKLDFKDRVQS KIGSLDNITHVPGGGNKKIETHKLTFRENAKAKTD HGAEIVYKSPVVSGDTSPRHLSNVSSTGSIDMVD SPQLATLADEVSASLAKQGL	E. Mylonas, A. Hascher, P. Bernado´, M. Blackledge, E. Mandelkow and D. I. Svergun, Biochemistry, 2008, 47, 10345– 10353.
Tau - K27	37	2	SSPGSPGTPGSRSRTPSLPTPPTREPKKVAVVR TPPKSPSSAKSRLQTAPVPMPDLKNVKSKIGSTE NLKHQPGGGSVQIVYKPVDLSKVTSKCGSLGNIH	E. Mylonas, A. Hascher, P. Bernado´, M. Blackledge, E. Mandelkow and D. I. Svergun,

			HKPGGGQVEVKSEKLDFKDRVQSKIGSLDNITHV PGGGNKKIETHKLTFRENAKAKTDHGAEIVY	Biochemistry, 2008, 47, 10345–10353.
Tau - K17	36	2	SSPGSPGTPGSRSRTPSLPTPPTREPKKVAVVR TPPKSPSSAKSRLQTAPVPMPDLKNVKSKIGSTE NLKHQPGGGSVQIVYKPVDLSKVTSKCGSLGNIH HKPGGGQVEVKSEKLDFKDRVQSKIGSLDNITHV PGGGNKKIE	E. Mylonas, A. Hascher, P. Bernado´, M. Blackledge, E. Mandelkow and D. I. Svergun, Biochemistry, 2008, 47, 10345–10353.
Tau - K19	35	1	QTAPVPMPDLKNVKSKIGSTENLKHQPGGGSVQ IVYKPVDLSKVTSKCGSLGNIHHKPGGGQVEVKS EKLDFKDRVQSKIGSLDNITHVPGGGNKKIE	E. Mylonas, A. Hascher, P. Bernado´, M. Blackledge, E. Mandelkow and D. I. Svergun, Biochemistry, 2008, 47, 10345–10353.
Tau - K44	52	2	MAEPRQEFEVMEDHAGTYGLGDRKDQGGYTM HQDQEGDTDAGLKAEEAGIGDTPSLEDEAAGHV TQARMVSKSKDGTGSDDKKAKGADGKTKIATPR GAAPPGQKGQANATRIPAKTPPAPKTPPSSGEP PKSGDRSGYSSPGSPGTPGSRSRTPSLPTPPTR EPKKVAVVRTPPKSPSSAKSRLQTAPVPMPDLK NVKSKIGSTENLKHQPGGGKVQIVYKPVDLSKVT SKCGSLGNIHHKPGGGQVEVKSEKLDFKDRVQS KIGSLDNITHVPGGGNKKIE	E. Mylonas, A. Hascher, P. Bernado´, M. Blackledge, E. Mandelkow and D. I. Svergun, Biochemistry, 2008, 47, 10345–10353.
Tau - K10	40	1	QTAPVPMPDLKNVKSKIGSTENLKHQPGGGSVQ IVYKPVDLSKVTSKCGSLGNIHHKPGGGQVEVKS EKLDFKDRVQSKIGSLDNITHVPGGGNKKIETHK LTFRENAKAKTDHGAEIVYKSPVVSGDTSPRHLS NVSSTGSIDMVDSPQLATLADEVSASLAKQGL	E. Mylonas, A. Hascher, P. Bernado´, M. Blackledge, E. Mandelkow and D. I. Svergun, Biochemistry, 2008, 47, 10345–10353.
Tau - K25	41	2	MAEPRQEFEVMEDHAGTYGLGDRKDQGGYTM HQDQEGDTDAGLKAEEAGIGDTPSLEDEAAGHV TQARMVSKSKDGTGSDDKKAKGADGKTKIATPR GAAPPGQKGQANATRIPAKTPPAPKTPPSSGEP PKSGDRSGYSSPGSPGTPGSRSRTPSLPTPPTR EPKKVAVVRTPPKSPSSAKSRL	E. Mylonas, A. Hascher, P. Bernado´, M. Blackledge, E. Mandelkow and D. I. Svergun, Biochemistry, 2008, 47, 10345–10353.

Tau - K23	49	2	MAEPRQEFEVMEDHAGTYGLGDRKDQGGYTM HQDQEGDTDAGLKAEEAGIGDTPSLEDEAAGHV TQARMVSKSKDGTGSDDKKAKGADGKTKIATPR GAAPPGQKGQANATRIPAKTPPAPKTPPSSGEP PKSGDRSGYSSPGSPGTPGSRSRTPSLPTPPTR EPKKVAVVRTPPKSPSSAKSRLKKIETHKLTFRE NAKAKTDHGAEIVYKSPVVSGDTSPRHLSNVSST GSIDMVDSPQLATLADEVSASLAKQGL	E. Mylonas, A. Hascher, P. Bernado´, M. Blackledge, E. Mandelkow and D. I. Svergun, Biochemistry, 2008, 47, 10345–10353.
Tau - K32 AT8 AT100	41	3	SEPGEPGEPGSRSREPELPTPPTREPKKVAVVR TPPKSPSSAKSRLQTAPVPMPDLKNVKSKIGSTE NLKHQPGGGKVQIINKKLDLSNVQSKCGSKDNIK HVPGGGSVQIVYKPVDLSKVTSKCGSLGNIHHKP GGGQVEVKSEKLDFKDRVQSKIGSLDNITHVPG GGNKKIETHKLTFRENAKAKTDHGAEIVY	E. Mylonas, A. Hascher, P. Bernado´, M. Blackledge, E. Mandelkow and D. I. Svergun, Biochemistry, 2008, 47, 10345–10353.
Tau - ht23 S214E	54	3	MAEPRQEFEVMEDHAGTYGLGDRKDQGGYTM HQDQEGDTDAGLKAEEAGIGDTPSLEDEAAGHV TQARMVSKSKDGTGSDDKKAKGADGKTKIATPR GAAPPGQKGQANATRIPAKTPPAPKTPPSSGEP PKSGDRSGYSSPGSPGTPGSRSRTPELPTPPTR EPKKVAVVRTPPKSPSSAKSRLQTAPVPMPDLK NVKSKIGSTENLKHQPGGGKVQIVYKPVDLSKVT SKCGSLGNIHHKPGGGQVEVKSEKLDFKDRVQS KIGSLDNITHVPGGGNKKIETHKLTFRENAKAKTD HGAEIVYKSPVVSGDTSPRHLSNVSSTGSIDMVD SPQLATLADEVSASLAKQGL	E. Mylonas, A. Hascher, P. Bernado´, M. Blackledge, E. Mandelkow and D. I. Svergun, Biochemistry, 2008, 47, 10345–10353.
Tau - ht23 AT8 AT100	52	3	MAEPRQEFEVMEDHAGTYGLGDRKDQGGYTM HQDQEGDTDAGLKAEEAGIGDTPSLEDEAAGHV TQARMVSKSKDGTGSDDKKAKGADGKTKIATPR GAAPPGQKGQANATRIPAKTPPAPKTPPSSGEP PKSGDRSGYSEPGEPGEPGSRSREPELPTPPTR EPKKVAVVRTPPKSPSSAKSRLQTAPVPMPDLK NVKSKIGSTENLKHQPGGGKVQIVYKPVDLSKVT SKCGSLGNIHHKPGGGQVEVKSEKLDFKDRVQS KIGSLDNITHVPGGGNKKIETHKLTFRENAKAKTD HGAEIVYKSPVVSGDTSPRHLSNVSSTGSIDMVD SPQLATLADEVSASLAKQGL	E. Mylonas, A. Hascher, P. Bernado´, M. Blackledge, E. Mandelkow and D. I. Svergun, Biochemistry, 2008, 47, 10345–10353.

Tau - K18 P301L	35	2	QTAPVPMPDLKNVKSKIGSTENLKHQPGGGKVQ IINKKLDLSNVQSKCGSKDNIKHVLGGGSVQIVYK PVDLSKVTSKCGSLGNIHHKPGGGQVEVKSEKL DFKDRVQSKIGSLDNITHVPGGGNKKIE	E. Mylonas, A. Hascher, P. Bernado´, M. Blackledge, E. Mandelkow and D. I. Svergun, Biochemistry, 2008, 47, 10345–10353.
Tau - K18 ΔK280	79	10	QTAPVPMPDLKNVKSKIGSTENLKHQPGGGKVQ IINKLDLSNVQSKCGSKDNIKHVLGGGSVQIVYKP VDLSKVTSKCGSLGNIHHKPGGGQVEVKSEKLD FKDRVQSKIGSLDNITHVPGGGNKKIE	E. Mylonas, A. Hascher, P. Bernado´, M. Blackledge, E. Mandelkow and D. I. Svergun, Biochemistry, 2008, 47, 10345–10353.
Tau - K18 ΔK280 I277P I308P	35	2	QTAPVPMPDLKNVKSKIGSTENLKHQPGGGKVQ PINKLDLSNVQSKCGSKDNIKHVLGGGSVQPVYK PVDLSKVTSKCGSLGNIHHKPGGGQVEVKSEKL DFKDRVQSKIGSLDNITHVPGGGNKKIE	E. Mylonas, A. Hascher, P. Bernado´, M. Blackledge, E. Mandelkow and D. I. Svergun, Biochemistry, 2008, 47, 10345–10353.
Histatin	13.2	0.01	DSHAKRHHGYKRKFHEKHHSHRGY	Cragnell, C., Durand, D., Cabane, B., and Skepö, M. (2016). Coarse-grained modeling of the intrinsically disordered protein Histatin 5 in solution: Monte Carlo simulations in combination with SAXS. Proteins 84, 777–791.
CortactinCR	46.7		GPLGSGYGGKFGVEQDRMDKSAVGHEYQSKLS KHCSQVDSVRGFGGKFGVQMDRVDQSAVGFEY QGKTEKHASQKDYSSGFGGKYGVQADRVDKSA VGFDYQGKTEKHESQRDYSKGFGGKYGIDKDK VDKSAVGFEYQGKTEKHESQKDYVKGFGGKFG VQTDRQDKCALGWDHQEKLQLHESQKDYKTGF GGKFGVQSERQDSAAVGFDYKEKLAKHESQQD YSKGFGGKYGVQKDRMDKNASTFEDVTQVSSA YQKTVPVEAVTSKTSNIRANFENLAKEKEQEDRR KAEAERAQRMAKERQEQEEARRKLEEQARAKT QT	Li, X., Tao, Y., Murphy, J.W., Scherer, A.N., Lam, T.T., Marshall, A.G., Koleske, A.J., and Boggon, T.J. (2017). The repeat region of cortactin is intrinsically disordered in solution. Sci. Rep. 7, 16696.

Pertactin-NTD	51.3	0.1	DWNNQSIVKTGERQHGIHIQGSDPGGVRTASGT TIKVSGRQAQGILLENPAAELQFRNGSVTSSGQL SDDGIRRFLGTVTVKAGKLVADHATLANVGDTW DDDGIALYVAGEQAQASIADSTLQGAGGVQIERG ANVTVQRSAIVDGGLHIGALQSLQPEDLPPSRVV LRDTNVTAVPASGAPAAVSVLGASELTLDGGHIT GGRAAGVAAMQGAVVHLQRATIRRGEALAGGA VPGGAVPGGAVPGGFGPGGFGPVLDGWYGVD VSGSSVELAQSIVEAPELGAAIRVGRGARVTVPG GSLSAPHGNVIETGGARRFAPQAAPLSITLQAGA H	Riback, J.A., Bowman, M.A., Zmyslowski, A.M., Knoverek, C.R., Jumper, J.M., Hinshaw, J.R., Kaye, E.B., Freed, K.F., Clark, P.L., and Sosnick, T.R. (2017). Innovative scattering analysis shows that hydrophobic disordered proteins are expanded in water. Science 358, 238–241.
Reduced_Rnase H	33.6	0.1	KETAAAKFERQHMDSSTSAASSSNYCNQMMKS RNLTKDRCKPVNTFVHESLADVQAVCSQKNVAC KNGQTNCYQSYSTMSITDCRETGSSKYPNCAYK TTQANKHIIVACEGNPYVPVHFDASV	Riback, J.A., Bowman, M.A., Zmyslowski, A.M., Knoverek, C.R., Jumper, J.M., Hinshaw, J.R., Kaye, E.B., Freed, K.F., Clark, P.L., and Sosnick, T.R. (2017). Innovative scattering analysis shows that hydrophobic disordered proteins are expanded in water. Science 358, 238–241.
Nup1573_frag	24	5	GCPSASPAFGANQTPTFGQSQGASQPNPPGFSI SSSTALFPTGSQPAPPTFGTVSSSSQPPVFGQQ PSQSAFGSTTPNA	Mercadante, D., Milles, S., Fuertes, G., Svergun, D.I., Lemke, E.A., and Gräter, F. (2015). Kirkwood-Buff Approach Rescues Overcollapse of a Disordered Protein in Canonical Protein Force Fields. J. Phys. Chem. B 119, 7975–7984.
LOX-PP	37	0.4	APPAAGQQQPPREPPAAPGAWRQQIQWENNG QVFSLLSLGSQYQPQRRRDPGAAVPGAANASA QQPRTPILLIRDNRTAAARTRTAGSSGVTAGRPR PTARHWFQAGYSTSRAREAGASRAENQTAPGE VPALSNLRPPSRVDGMVG	Vallet, S.D., Miele, A.E., Uciechowska-Kaczmarzyk, U., Liwo, A., Duclos, B., Samsonov, S.A., and Ricard-Blum, S. (2018). Insights into the structure and dynamics of lysyl oxidase propeptide, a

				flexible protein with numerous partners. Sci. Rep. 8, 11768.
H1_CTD	25	0.2	KGDEPKRSVAFKKTKKEVKKVATPKKAAKPKKA ASKAPSKKPKATPVKKAKKKPAATPKKAKKPKVV KVKPVKASKPKKAKTVKPKAKSSAKRASKKK	Roque, A., Ponte, I., and Suau, P. (2007). Macromolecular crowding induces a molten globule state in the C-terminal domain of histone H1. Biophys. J. 93, 2170–2177.
p27_WT (v31)	28.1	1.8	GSHMKGACKVPAQESQDVSGSRPAAPLIGAPAN SEDTHLVDPKTDPSDSQTGLAEQCAGIRKRPAT DDSSTQNKRANRTEENVSDGSPNAGSVEQTPK KPGLRRRQT	Das, R.K., Huang, Y., Phillips, A.H., Kriwacki, R.W., and Pappu, R.V. (2016). Cryptic sequence features within the disordered protein p27Kip1 regulate cell cycle signaling. Proc. Natl. Acad. Sci. U. S. A. 113, 5616–5621.
p27_v14	29.4	1.3	GSHMKGACKSSSPPSNDQGRPGDPKQVIDKTE VERTQDTSNIQETQSANNSGPDKPSRCDLAVSG VAAAALPAPGHANSTARDLTRDEEAGSVEQTPK KPGLRRRQT	Das, R.K., Huang, Y., Phillips, A.H., Kriwacki, R.W., and Pappu, R.V. (2016). Cryptic sequence features within the disordered protein p27Kip1 regulate cell cycle signaling. Proc. Natl. Acad. Sci. U. S. A. 113, 5616–5621.
p27_v15	29.2	1	GSHMKGACIVANSPPDDVKSKEDVPQTDPRLTG GDRDNARASRTGNDPAGASTQSAEVACSNPILS TPDAQEKQAGTSNSKERPHEQLSAGSVEQTPKK PGLRRRQT	Das, R.K., Huang, Y., Phillips, A.H., Kriwacki, R.W., and Pappu, R.V. (2016). Cryptic sequence features within the disordered protein p27Kip1 regulate cell cycle signaling. Proc. Natl. Acad. Sci. U. S. A. 113, 5616–5621.
p27_v44	24.9	1.3	GSHMKGACRKPANAEADSSSCQNVPRGKSKQA PETPTGSPLGDATLNQVKPRRPSSASTNIGQLED	Das, R.K., Huang, Y., Phillips, A.H., Kriwacki, R.W., and Pappu, R.V. (2016). Cryptic

			ADEDDAEDHVGSAVTSQTIPNDRAGSVEQTPKKPGLRRRQT	sequence features within the disordered protein p27Kip1 regulate cell cycle signaling. Proc. Natl. Acad. Sci. U. S. A. 113, 5616–5621.
p27_v56	23.3	1	GSHMKGACGSSVLGTGNPRNQAHVSDTSLEEDDDEQDDSTPDEVSQACTIVASALDINAATPRSPKASPKRKRKRQSTAPAQGNEPPGNAGSVEQTPKKPGLRRRQT	Das, R.K., Huang, Y., Phillips, A.H., Kriwacki, R.W., and Pappu, R.V. (2016). Cryptic sequence features within the disordered protein p27Kip1 regulate cell cycle signaling. Proc. Natl. Acad. Sci. U. S. A. 113, 5616–5621.
p27_v78	22.1	0.3	GSHMKGACALPSGVVPAEDDDDDEEEEDDQDPAQPQAVQGAAPSSGTNNSQPILPSIAVNSTTGPNSTAGKKKRKRRRTRHSNCATLSSAGSVEQTPKKPGLRRRQT	Das, R.K., Huang, Y., Phillips, A.H., Kriwacki, R.W., and Pappu, R.V. (2016). Cryptic sequence features within the disordered protein p27Kip1 regulate cell cycle signaling. Proc. Natl. Acad. Sci. U. S. A. 113, 5616–5621.
Ki-1/57	47	2	PRRGEQQGWNDSRGPEGMLERAERRSYREYRPYETERQADFTAEKFPDEKPGDRFDRDRPLRGRGGPRGGMRGRGRGGPGNRVFDAFDQRGKREFERYGGNDKIAVRTEDNMGGCGVRTWGSGKDTSDVEPTAPMEEPTVVEESQGTPEEESPAKVPELEVEEETQVQEMTLDEWKNLQEQTRPKPEFNIRKPESTVPSKAVVIHKSKYRDDMVKDDYEDDSHVFRKPANDITSQLEINFGNLPRPGRGARGGTRGGRGRIRRAENYGPRAEVVMQDVAPNPDDPEDFPALS	Bressan, G.C., Silva, J.C., Borges, J.C., Dos Passos, D.O., Ramos, C.H.I., Torriani, I.L., and Kobarg, J. (2008). Human regulatory protein Ki-1/57 has characteristics of an intrinsically unstructured protein. J. Proteome Res. 7, 4465–4474.
CTCF-R domain (WT)	32.5	1.8	SAERRNSILTETLHRFSLEGDAPVSWTETKKQSFKQTGEFGEKRKNSILNPINSIRKFSIVQKTPLQMNGIEEDSDEPLERRLSLVPDSEQGEAILPRISVISTGPTLQARRRQSVLNLMTHSVNQGQNIHRKTTASTRKVSLAPQANLTELDIYSRRLSQETGLEISEEINEEDLKECFFDDME	Marasini, C., Galeno, L., and Moran, O. (2013). A SAXS-based ensemble model of the native and phosphorylated regulatory domain of the CFTR. Cell. Mol. Life Sci. 70, 923–933.

CTCF-R domain (phosphorylated)	29.2	0.4	SAERRNSILTETLHRFSLEGDAPVSWTETKKQSF KQTGEFGEKRKNSILNPINSIRKFSIVQKTPLQMN GIEEDSDEPLERRLSLVPDSEQGEAILPRISVIST GPTLQARRRQSVLNLMTHSVNQGQNIHRKTTAS TRKVSLAPQANLTELDIYSRRLSQETGLEISEEIN EEDLKECFFDDME	Marasini, C., Galeno, L., and Moran, O. (2013). A SAXS-based ensemble model of the native and phosphorylated regulatory domain of the CFTR. Cell. Mol. Life Sci. 70, 923–933.
hNHE1cdt	37.5	0	VPAHKLDSPTMSRARIGSDPLAYEPKEDLPVITID PASPQSPESVDLVNEELKGKVLGLSRDPAKVAE EDEDDDGGIMMRSKETSSPGTDDVFTPAPSDSP SSQRIQRCLSDPGPHPEPGEGEPFFPKGQ	Kjaergaard, M., Nørholm, A.-B., Hendus-Altenburger, R., Pedersen, S.F., Poulsen, F.M., and Kragelund, B.B. (2010). Temperature-dependent structural changes in intrinsically disordered proteins: Formation of α-helices or loss of polyproline II? Protein Sci. 19, 1555–1564.
pMBP	54	0	ASQKRPSQRHGSKYLASASTMDHARHGFLPRH RDTGIDSLGRFFGADRGAPKRGSGKDGHHAAR TTHYGSLPQKAQHGRPQDENPVVHFFKNIVTPR TPPPSQGKGRGLSLSRFSWGAEGQKPGFGYGG RAPDYKPAHKGLKGAQDAQGTLSKIFKLGGRDS RSGSPMARR	Majava, V., Wang, C., Myllykoski, M., Kangas, S.M., Kang, S.U., Hayashi, N., Baumgärtel, P., Heape, A.M., Lubec, G., and Kursula, P. (2010). Structural analysis of the complex between calmodulin and full-length myelin basic protein, an intrinsically disordered molecule. Amino Acids 39, 59–71.
HMPV	27.4	0.5	MSFPEGKDILFMGNEAAKLAEAFQKSLRKPSHK RSQSIIGEKVNTVSETLELPTISRPTKP	Renner, M., Paesen, G.C., Grison, C.M., Granier, S., Grimes, J.M., and Leyrat, C. (2017). Structural dissection of human metapneumovirus phosphoprotein using small angle x-ray scattering. Sci. Rep. 7, 14865.

redAFP	22.2	0.1	CKGADGAHGVNGCPGTAGAAGSVGGPGCDGG HGGNGGNGNPGCAGGVGGAGGASGGTGVGG RGGKGGSGTPKGADGAPGAP	Gates, Z.P., Baxa, M.C., Yu, W., Riback, J.A., Li, H., Roux, B., Kent, S.B.H., and Sosnick, T.R. (2017). Perplexing cooperative folding and stability of a low-sequence complexity, polyproline 2 protein lacking a hydrophobic core. Proc. Natl. Acad. Sci. U. S. A. 114, 2241–2246.
CSD1 (with overhang)	35.4	0	MAMITNSSSVPAESKSSKPSGKSDMDAALDDLID TLGGPEETEEDNTTYTGPEVLDPMSSTYIEELGK REVTLPPKYRELLDKKEGIPVPPPDTSKPLGPDD AIDALSLDLTCSSPTADGKKTEKEKSTGEVLKAQ SVGVIKSDPLESLN	Konno, T., Tanaka, N., Kataoka, M., Takano, E., and Maki, M. (1997). A circular dichroism study of preferential hydration and alcohol effects on a denatured protein, pig calpastatin domain I. Biochim. Biophys. Acta 1342, 73–82.
PAGE4_WT	36.2	1.1	MSARVRSRSRGRGDGQEAPDVVAFVAPGESQQ EEPPTDNQDIEPGQEREGTPPIEERKVEGDCQE MDLEKTRSERGDGSDVKEKTPPNPKHAKTKEAG DGQP	Kulkarni, P., Jolly, M.K., Jia, D., Mooney, S.M., Bhargava, A., Kagohara, L.T., Chen, Y., Hao, P., He, Y., Veltri, R.W., et al. (2017). Phosphorylation-induced conformational dynamics in an intrinsically disordered protein and potential role in phenotypic heterogeneity. Proc. Natl. Acad. Sci. U. S. A. 114, E2644–E2653.
PAGE4_WT_pho sphorylated	49.8	1.9	MSARVRSRSRGRGDGQEAPDVVAFVAPGESQQ EEPPTDNQDIEPGQEREGTPPIEERKVEGDCQE MDLEKTRSERGDGSDVKEKTPPNPKHAKTKEAG DGQP	Kulkarni, P., Jolly, M.K., Jia, D., Mooney, S.M., Bhargava, A., Kagohara, L.T., Chen, Y., Hao, P., He, Y., Veltri, R.W., et al. (2017). Phosphorylation-induced conformational dynamics in an intrinsically disordered protein and potential

				role in phenotypic heterogeneity. Proc. Natl. Acad. Sci. U. S. A. 114, E2644–E2653.
ERalpha-NTD	31	0.2	SNAMTMTLHTKASGMALLHQIQGNELEPLNRPQ LKIPLERPLGEVYLDSSKPAVYNYPEGAAYEFNA AAAANAQVYGQTGLPYGPGSEAAAFGSNGLGG FPPLNSVSPSPLMLLHPPPQLSPFLQPHGQQVP YYLENEPSGYTVREAGPPAFYRPNSDNRRQGG RERLASTNDKGSMAMESAKETRY	Peng, Y., Cao, S., Kiselar, J., Xiao, X., Du, Z., Hsieh, A., Ko, S., Chen, Y., Agrawal, P., Zheng, W., Shi, W., Jiang, W., Yang, L., Chance, M. R., Surewicz, W. K., Buck, M., & Yang, S. (2019). A Metastable Contact and Structural Disorder in the Estrogen Receptor Transactivation Domain. Structure , 27(2), 229–240.e4.
A1-LCD-NLS	27.6	0.16	GSMASASSSQRGRSGSGNFGGGRGGGFGGND NFGRGGNFSGRGGFGGSRGGGGYGGSGDGY NGFGNDGSNFGGGGSYNDFGNYNNQSSNFGP MKGGNFGGRSSGGSGGGGQYFAKPRNQGGYG GSSSSSSYGSGRRF	Bremer, A., Farag, M., Borcherds, W. M., Peran, I., Martin, E. W., Pappu, R. V., & Mittag, T. (2022). Deciphering how naturally occurring sequence features impact the phase behaviours of disordered prion-like domains. Nature Chemistry, 14(2), 196–207.
A1-LCD+NLS	25.83	0.11	GSMASASSSQRGRSGSGNFGGGRGGGFGGND NFGRGGNFSGRGGFGGSRGGGGYGGSGDGY NGFGNDGSNFGGGGSYNDFGNYNNQSSNFGP MKGGNFGGRSSGPYGGGGQYFAKPRNQGGYG GSSSSSSYGSGRRF	Bremer, A., Farag, M., Borcherds, W. M., Peran, I., Martin, E. W., Pappu, R. V., & Mittag, T. (2022). Deciphering how naturally occurring sequence features impact the phase behaviours of disordered prion-like domains. Nature Chemistry, 14(2), 196–207.
A1-LCD-12F+12Y	26.04	0.2	GSMASASSSQRGRSGSGNYGGGRGGGYGGND NYGRGGNYSGRGGYGGSRGGGGYGGSGDGY NGYGNDGSNYGGGGSYNDYGNYNNQSSNYGP	Bremer, A., Farag, M., Borcherds, W. M., Peran, I., Martin, E. W., Pappu, R. V., & Mittag, T. (2022). Deciphering

			MKGGNYGGRSSGGSGGGGQYYAKPRNQGGY GGSSSSSSYGSGRRY	how naturally occurring sequence features impact the phase behaviours of disordered prion-like domains. Nature Chemistry, 14(2), 196–207.
A1-LCD+7F-7Y	27.18	0.13	GSMASASSSQRGRSGSGNFGGGRGGGFGGND NFGRGGNFSGRGGFGGSRGGGGFGGSGDGFN GFGNDGSNFGGGGSFNDFGNFNNQSSNFGPM KGGNFGGRSSGGSGGGGQFFAKPRNQGGFGG SSSSSSFGSGRRF	Bremer, A., Farag, M., Borcherds, W. M., Peran, I., Martin, E. W., Pappu, R. V., & Mittag, T. (2022). Deciphering how naturally occurring sequence features impact the phase behaviours of disordered prion-like domains. Nature Chemistry, 14(2), 196–207.
A1-LCD-9F+6Y	26.55	0.1	GSMASASSSQRGRSGSGNFGGGRGGGYGGND NYGRGGNYSGRGGFGGSRGGGGYGGSGDGY NGGGNDGSNYGGGGSYNDSGNYNNQSSNFGP MKGGNYGGRSSGGSGGGGQYGAKPRNQGGY GGSSSSSSYGSGRRY	Bremer, A., Farag, M., Borcherds, W. M., Peran, I., Martin, E. W., Pappu, R. V., & Mittag, T. (2022). Deciphering how naturally occurring sequence features impact the phase behaviours of disordered prion-like domains. Nature Chemistry, 14(2), 196–207.
A1-LCD-8F+4Y	27.07	0.07	GSMASASSSQRGRSGSGNFGGGRGGGYGGND NGGRGGNYSGRGGFGGSRGGGGYGGSGDGY NGGGNDGSNYGGGGSYNDSGNYNNQSSNFGP MKGGNYGGRSSGGSGGGGQYGAKPRNQGGY GGSSSSSSYGSGRRF	Bremer, A., Farag, M., Borcherds, W. M., Peran, I., Martin, E. W., Pappu, R. V., & Mittag, T. (2022). Deciphering how naturally occurring sequence features impact the phase behaviours of disordered prion-like domains. Nature Chemistry, 14(2), 196–207.
A1-LCD-9F+3Y	26.83	0.13	GSMASASSSQRGRSGSGNFGGGRGGGYGGND NGGRGGNYSGRGGFGGSRGGGGYGGSGDGY NGGGNDGSNYGGGGSYNDSGNGNNQSSNFGP	Bremer, A., Farag, M., Borcherds, W. M., Peran, I., Martin, E. W., Pappu, R. V., & Mittag, T. (2022). Deciphering how naturally occurring

			MKGGNYGGRSSGGSGGGGQYGAKPRNQGGY GGSSSSSSYGSGRRS	sequence features impact the phase behaviours of disordered prion-like domains. Nature Chemistry, 14(2), 196–207.
A1-LCD-10R	26.71	0.07	GSMASASSSQGGSSGSGNFGGGGGGGFGGND NFGGGGNFSGSGGFGGSGGGGGYGGSGDGY NGFGNDGSNFGGGGSYNDFGNYNNQSSNFGP MKGGNFGGSSSGPYGGGGGQYFAKPGNQGGYG GSSSSSSYGSGGGF	Bremer, A., Farag, M., Borcherds, W. M., Peran, I., Martin, E. W., Pappu, R. V., & Mittag, T. (2022). Deciphering how naturally occurring sequence features impact the phase behaviours of disordered prion-like domains. Nature Chemistry, 14(2), 196–207.
A1-LCD-6R	25.73	0.09	GSMASASSSQGGRSGSGNFGGGRGGGFGGND NFGGGGNFSGSGGFGGSRGGGGYGGSGDGY NGFGNDGSNFGGGGSYNDFGNYNNQSSNFGP MKGGNFGGSSSGPYGGGGGQYFAKPGNQGGYG GSSSSSSYGSGGRF	Bremer, A., Farag, M., Borcherds, W. M., Peran, I., Martin, E. W., Pappu, R. V., & Mittag, T. (2022). Deciphering how naturally occurring sequence features impact the phase behaviours of disordered prion-like domains. Nature Chemistry, 14(2), 196–207.
A1-LCD+2R	26.23	0.23	GSMASASSSQRGRSGSGNFGGGRGGGFGGND NFGRGGNFSGRGGFGGSRGGGGYGGSGDGY NGFRNDGSNFGGGGRYNDFGNYNNQSSNFGP MKGGNFGGRSSGPYGGGGGQYFAKPRNQGGYG GSSSSSSYGSGRRF	Bremer, A., Farag, M., Borcherds, W. M., Peran, I., Martin, E. W., Pappu, R. V., & Mittag, T. (2022). Deciphering how naturally occurring sequence features impact the phase behaviours of disordered prion-like domains. Nature Chemistry, 14(2), 196–207.
A1-LCD+7R	27.09	0.07	GSMASASSSQRGRSGRGNFGGGRGGGFGGND NFGRGGNFSGRGGFGGSRGGGRYGGSGDRYN GFGNDGRNFGGGGSYNDFGNYNNQSSNFGPM KGGNFRGRSSGPYGRGGQYFAKPRNQGGYGG SSSSRSYGSGRRF	Bremer, A., Farag, M., Borcherds, W. M., Peran, I., Martin, E. W., Pappu, R. V., & Mittag, T. (2022). Deciphering how naturally occurring sequence features impact the

				phase behaviours of disordered prion-like domains. Nature Chemistry, 14(2), 196–207.
A1-LCD-3R+3K	26.34	0.15	GSMASASSSQRGKSGSGNFGGGRGGGFGGND NFGRGGNFSGRGGFGGSKGGGGYGGSGDGYN GFGNDGSNFGGGGSYNDFGNYNNQSSNFGPM KGGNFGGRSSGGSGGGGGQYFAKPRNQGGYGG SSSSSSYGSGRKF	Bremer, A., Farag, M., Borcherds, W. M., Peran, I., Martin, E. W., Pappu, R. V., & Mittag, T. (2022). Deciphering how naturally occurring sequence features impact the phase behaviours of disordered prion-like domains. Nature Chemistry, 14(2), 196–207.
A1-LCD-6R+6K	27.87	0.08	GSMASASSSQKGKSGSGNFGGGRGGGFGGND NFGKGGNFSGRGGFGGSKGGGGYGGSGDGYN GFGNDGSNFGGGGSYNDFGNYNNQSSNFGPM KGGNFGGKSSGGSGGGGGQYFAKPRNQGGYGG SSSSSSYGSGRKF	Bremer, A., Farag, M., Borcherds, W. M., Peran, I., Martin, E. W., Pappu, R. V., & Mittag, T. (2022). Deciphering how naturally occurring sequence features impact the phase behaviours of disordered prion-like domains. Nature Chemistry, 14(2), 196–207.
A1-LCD-10R+10K	28.49	0.05	GSMASASSSQKGKSGSGNFGGGKGGGFGGND NFGKGGNFSGKGGFGGSKGGGGYGGSGDGYN GFGNDGSNFGGGGSYNDFGNYNNQSSNFGPM KGGNFGGKSSGGSGGGGGQYFAKPKNQGGYGG SSSSSSYGSGKKF	Bremer, A., Farag, M., Borcherds, W. M., Peran, I., Martin, E. W., Pappu, R. V., & Mittag, T. (2022). Deciphering how naturally occurring sequence features impact the phase behaviours of disordered prion-like domains. Nature Chemistry, 14(2), 196–207.
A1-LCD-4D	26.42	0.12	GSMASASSSQRGRSGSGNFGGGRGGGFGGNG NFGRGGNFSGRGGFGGSRGGGGYGGSGGGY NGFGNSGSNFGGGGSYNGFGNYNNQSSNFGP MKGGNFGGRSSGPYGGGGQYFAKPRNQGGYG GSSSSSSYGSGRRF	Bremer, A., Farag, M., Borcherds, W. M., Peran, I., Martin, E. W., Pappu, R. V., & Mittag, T. (2022). Deciphering how naturally occurring sequence features impact the phase behaviours of disordered

				prion-like domains. Nature Chemistry, 14(2), 196–207.
A1-LCD+4D	27.18	0.3	GSMASASSSQRDRSGSGNFGGGRGGGFGGND NFGRGGNFSGRGDFGGSRGGGGYGGSGDGYN GFGNDGSNFGGGGSYNDFGNYNNQSSNFGPM KGGNFGGRSSDPYGGGGQYFAKPRNQGGYGG SSSSSSSYDSGRRF	Bremer, A., Farag, M., Borcherds, W. M., Peran, I., Martin, E. W., Pappu, R. V., & Mittag, T. (2022). Deciphering how naturally occurring sequence features impact the phase behaviours of disordered prion-like domains. Nature Chemistry, 14(2), 196–207.
A1-LCD+8D	26.85	0.07	GSMASASSSQRDRSGSGNFGGGRDGGFGGND NFGRGDNFSGRGDFGGSRDGGGYGGSGDGYN GFGNDGSNFGGGGSYNDFGNYNNQSSNFGPM KGGNFGGRSSDPYGGGGQYFAKPRNQDGYGG SSSSSSSYDSGRRF	Bremer, A., Farag, M., Borcherds, W. M., Peran, I., Martin, E. W., Pappu, R. V., & Mittag, T. (2022). Deciphering how naturally occurring sequence features impact the phase behaviours of disordered prion-like domains. Nature Chemistry, 14(2), 196–207.
A1-LCD+12D	28.01	0.12	GSMASADSSQRDRDDSGNFGDGRGGGFGGND NFGRGGNFSDRGGFGGSRGDGGYGGDGDGYN GFGNDGSNFGGGGSYNDFGNYNNQSSNFDPM KGGNFGDRSSGPYDGGGQYFAKPRNQGGYGG SSSSSSSYGSDRRF	Bremer, A., Farag, M., Borcherds, W. M., Peran, I., Martin, E. W., Pappu, R. V., & Mittag, T. (2022). Deciphering how naturally occurring sequence features impact the phase behaviours of disordered prion-like domains. Nature Chemistry, 14(2), 196–207.
A1-LCD+12E	28.52	0.05	GSMASAESSQREREESGNFGEGRGGGFGGND NFGRGGNFSERGGFGGSRGEGGYGGEGDGYN GFGNDGSNFGGGGSYNDFGNYNNQSSNFEPM KGGNFGERSSGPYEGGGQYFAKPRNQGGYGG SSSSSSSYGSERRF	Bremer, A., Farag, M., Borcherds, W. M., Peran, I., Martin, E. W., Pappu, R. V., & Mittag, T. (2022). Deciphering how naturally occurring sequence features impact the phase behaviours of disordered

				prion-like domains. Nature Chemistry, 14(2), 196–207.
A1-LCD+7R+10D	29.21	0.08	GSMASADSSQRDRDGRGNFGDGRGGGFGGND NFGRGGNFSDRGGFGGSRGGGRYGGDGDRYN GFGNDGRNFGGGGSYNDFGNYNNQSSNFDPM KGGNFRDRSSGPYDRGGQYFAKPRNQGGYGG SSSSRSYGSDRRF	Bremer, A., Farag, M., Borcherds, W. M., Peran, I., Martin, E. W., Pappu, R. V., & Mittag, T. (2022). Deciphering how naturally occurring sequence features impact the phase behaviours of disordered prion-like domains. Nature Chemistry, 14(2), 196–207.
A1-LCD+7K+12Dblocky	25.62	0.14	GSMASAKSSQRDRDDDGNFGKGRGGGFGGNK NFGRGGNFSKRGGFGGSRGKGKYGGKGDDYN GFGNDGDNFGGGGSYNDFGNYNNQSSNFDPM DGGNFDDRSSGPYDDGGQYFADPRNQGGYGG SSSSKSYGSKRRF	Bremer, A., Farag, M., Borcherds, W. M., Peran, I., Martin, E. W., Pappu, R. V., & Mittag, T. (2022). Deciphering how naturally occurring sequence features impact the phase behaviours of disordered prion-like domains. Nature Chemistry, 14(2), 196–207.
A1-LCD-12F+12Y10R	26.07	0.2	GSMASASSSQGGSSGSGNYGGGGGGGYGGN DNYGGGGNYSGSGGYGGSGGGGGYGGSGDG YNGYGNDGSNYGGGGSYNDYGNYNNQSSNYG PMKGGNYGGSSSGPYGGGGQYYAKPGNQGGY GGSSSSSSYGSGGGY	Bremer, A., Farag, M., Borcherds, W. M., Peran, I., Martin, E. W., Pappu, R. V., & Mittag, T. (2022). Deciphering how naturally occurring sequence features impact the phase behaviours of disordered prion-like domains. Nature Chemistry, 14(2), 196–207.
A1-LCD10F+7R+12D	28.6	0.04	GSMASADSSQRDRDDRGNFGDGRGGGGGGN DNFGRGGNGSDRGGGGGSRGDGRYGGDGDR YNGGGNDGRNGGGGGSYNDGGNYNNQSSNG DPMKGGNGRDRSSGPYDRGGQYGAKPRNQGG YGGSSSSRSYGSDRRG	Bremer, A., Farag, M., Borcherds, W. M., Peran, I., Martin, E. W., Pappu, R. V., & Mittag, T. (2022). Deciphering how naturally occurring sequence features impact the phase behaviours of disordered

				prion-like domains. Nature Chemistry, 14(2), 196–207.
PNt	51.1	0.13	DWNNQSIVKTGERQHGIHIQGSDPGGVRTASGTTIKVSGRQAQGILLENPAAELQFRNGSVTSSGQLSDDGIRRFLGTVTVKAGKLVADHATLANVGDTWDDDGIALYVAGEQAQASIADSTLQGAGGVQIERGANVTVQRSAIVDGGLHIGALQSLQPEDLPPSRVVLRDTNVTAVPASGAPAAVSVLGASELTLDGGHITGGRAAGVAAMQGAVVHLQRATIRRGEALAGGAVPGGAVPGGAVPGGFGPGGFGPVLDGWYGVDVSGSSVELAQSIVEAPELGAAIRVGRGARVTVPGGSLSAPHGNVIETGGARRFAPQAAPLSITLQAGAH	Bowman, M. A., Riback, J. A., Rodriguez, A., Guo, H., Li, J., Sosnick, T. R., & Clark, P. L. (2020). Properties of protein unfolded states suggest broad selection for expanded conformational ensembles. Proceedings of the National Academy of Sciences, 117(38), 23356–23364.
Swap1	49.2	0.59	DWNNQSIVKTGERQHGIHIQGSDPGGVRTASGTTIKVSGRQAQGILLENPAAELQFRNGSVTSSGQKSDDGIRRFLGTVTVLAGKLVADHATLANVGDTWDDDGIALYVAGEQAQASIADSTLQGAGGVQIERGANVTVQRSAIVLGGLHIGALQSLQPEDDPPSRVVLRDTNVTAVPASGAPAAVSVLGASLLTLDGGHITGGRAAGVAAMQGAVVHEQRATIRRGEALAGGAVPGGAVPGGAVPGGFGPGGFGPVLDGWYGVDVSGSSVELAQSIVEAPELGAAIRVGRGARVTVPGGSLSAPHGNVIETGGARRFAPQAAPLSITLQAGAH	Bowman, M. A., Riback, J. A., Rodriguez, A., Guo, H., Li, J., Sosnick, T. R., & Clark, P. L. (2020). Properties of protein unfolded states suggest broad selection for expanded conformational ensembles. Proceedings of the National Academy of Sciences, 117(38), 23356–23364.
Swap3	40.58	1.07	DWNNQSIVKTGERQHGIHIQGSDPGGVRTASGTTIKVSGRQAQGILLENPAAELQFRNGSVTSSGQKSTDGTRRFLGDVIVKAGLLVADHATLANVGDTWDDDGIALYVAGEQAQASIADSTLQGAGGVQIERGANVDVLRLAIVDGGLHIGALQSQQPETSPPSRVVLRDTNVTAVPASGAPAAVSVQGASEQTLDGGAITGGRAAGVAAMLGHVVHLLRATIRRGEALAGGAVPGGAVPGGAVPGGFGPGGFGPVLDGWYGVDVSGSSVELAQSIVEAPELGAAIRVGRGARVTVPGGSLSAPHGNVIETGGARRFAPQAAPLSITLQAGAH	Bowman, M. A., Riback, J. A., Rodriguez, A., Guo, H., Li, J., Sosnick, T. R., & Clark, P. L. (2020). Properties of protein unfolded states suggest broad selection for expanded conformational ensembles. Proceedings of the National Academy of Sciences, 117(38), 23356–23364.
Swap4	53.37	0.17	DWNNQSIVKTGERQHGIHIQGSDPGGVRTASGTTIKVSGRQAQGILLENPAAELQFRNGSVTSSGQL	Bowman, M. A., Riback, J. A., Rodriguez, A., Guo, H., Li, J.,

			SFVGITRDLGRDTVKAGKLVADHATLANVGDTW DDDGIALYVAGEQAQASIADSTLQGAGGVQIERG ADVRVQREAIVDGGLHNGALQSLQPSILPPSTVV LRDTNVTAVPASGAPAAVLVSGASGLRLDGGHI HEGRAAGVAAMQGAVVTLQTATIRRGEALAGGA VPGGAVPGGAVPGGFGPGGFGPVLDGWYGVD VSGSSVELAQSIVEAPELGAAIRVGRGARVTVPG GSLSAPHGNVIETGGARRFAPQAAPLSITLQAGA H	Sosnick, T. R., & Clark, P. L. (2020). Properties of protein unfolded states suggest broad selection for expanded conformational ensembles. Proceedings of the National Academy of Sciences, 117(38), 23356–23364.
Swap4.1	54.45	0.14	DWNNQSIVKTGERQHGIHIQGSDPGGVRTASGT TIKVSGRQAQGILLENPAAELQFRNGSVTSSGQL SFVGITRRLGDDTVKAGKLVADHATLANVGDTW DDDGIALYVAGEQAQASIADSTLQGAGGVQIERG ADVEVQRRAIVDGGLHNGALQSLQPSILPPSTVV LRDTNVTAVPASGAPAAVLVSGASGLELDGGHIH RGRAAGVAAMQGAVVTLQTATIRRGEALAGGAV PGGAVPGGAVPGGFGPGGFGPVLDGWYGVDV SGSSVELAQSIVEAPELGAAIRVGRGARVTVPGG SLSAPHGNVIETGGARRFAPQAAPLSITLQAGAH	Bowman, M. A., Riback, J. A., Rodriguez, A., Guo, H., Li, J., Sosnick, T. R., & Clark, P. L. (2020). Properties of protein unfolded states suggest broad selection for expanded conformational ensembles. Proceedings of the National Academy of Sciences, 117(38), 23356–23364.
Swap5	48.71	0.34	DWNNQSIVKTGERQHGIHIQGSDPGGVRTASGT TIKVSGRQAQGILLENPAAELQFRNGSVTSSGQL SDDGIEDFLGTVTVDAGELVADHATLANVGDTW DDDGIALYVAGEQAQASIADSTLQGAGGVQIEDG ANVTVQESAIVDGGLHIGALQSLQPRRLPPSRVV LRKTNVTAVPASGAPAAVSVLGASKLTLRGGHIT GGRAAGVAAMQGAVVHLQRATIRRGRALAGGA VPGGAVPGGAVPGGFGPGGFGPVLDGWYGVD VSGSSVELAQSIVEAPELGAAIRVGRGARVTVPG GSLSAPHGNVIETGGARRFAPQAAPLSITLQAGA H	Bowman, M. A., Riback, J. A., Rodriguez, A., Guo, H., Li, J., Sosnick, T. R., & Clark, P. L. (2020). Properties of protein unfolded states suggest broad selection for expanded conformational ensembles. Proceedings of the National Academy of Sciences, 117(38), 23356–23364.
Swap6	52.61	0.27	DWNNQSIVKTGERQHGIHIQGSDPGGVRTASGT TIKVSGRQAQGILLENPAAELQFRNGSVTSSGQL SDRGIDRFLGTVTVEAGKLVADHATLANVGDTW DKDGIALYVAGRQAQASIADSTLQGAGGVQIREG ANVTVQRSAIVDGGLHIGALQSLQPERLPPSDVV LRDTNVTAVPASGAPAAVSVLGASRLTLDGGHIT GGDAAGVAAMQGAVVHLQRATIERGEALAGGA VPGGAVPGGAVPGGFGPGGFGPVLDGWYGVD VSGSSVELAQSIVEAPELGAAIRVGRGARVTVPG	Bowman, M. A., Riback, J. A., Rodriguez, A., Guo, H., Li, J., Sosnick, T. R., & Clark, P. L. (2020). Properties of protein unfolded states suggest broad selection for expanded conformational ensembles. Proceedings of the National

			GSLSAPHGNVIETGGARRFAPQAAPLSITLQAGAH	Academy of Sciences, 117(38), 23356–23364.
sfAFP	23.1	2	CKGADGAHGVNGCPGTAGAAGSVGGPGCDGGHGGNGGNGNPGCAGGVGGAGGASGGTGVGGRGGKGGSGTPKGADGAPGAP	Gates ZP, Baxa MC, Yu W, Riback JA, Li H, Roux B, et al. Perplexing cooperative folding and stability of a low-sequence complexity, polyproline 2 protein lacking a hydrophobic core. Proc Natl Acad Sci U S A. 2017;114: 2241–2246.
FCP1	15.6	0.12	ESSRESSNEDEGSSSEADEMAKALEAELNDLM	Gibbs, Eric B., and Scott A. Showalter. 2016. "Quantification of Compactness and Local Order in the Ensemble of the Intrinsically Disordered Protein FCP1." The Journal of Physical Chemistry. B 120 (34): 8960–69.
RS-peptide	12.62	0.07	MYRSRSRSRSRSRSRSRS	**SAXS data – NMR data - Xiang, S., Gapsys, V., Kim, H.-Y., Bessonov, S., Hsiao, H.-H., Möhlmann, S., Klaukien, V., Ficner, R., Becker, S., Urlaub, H., Lührmann, R., de Groot, B., & Zweckstetter, M. (2013). Phosphorylation drives a dynamic switch in serine/arginine-rich proteins. Structure , 21(12), 2162–2174.**
P1_100	29	0	MAEEQARHVKNGLECIRALKAEPIGSLAIEEAMAAWSEISDNPGQERATCREEKAGSSGLSKPCLSAIGSTEGGAPRIRGQGPGESDDDAETLGIPPRNL	Naudi-Fabra, S., Tengo, M., Jensen, M. R., Blackledge, M., & Milles, S. (2021). Quantitative Description of Intrinsically Disordered Proteins Using Single-Molecule FRET, NMR, and SAXS. Journal of the

				American Chemical Society, 143(48), 20109–20121.
DSS1	25	0.1	MSRAALPSLENLEDDDEFEDFATENWPMKDTEL DTGDDTLWENNWDDEDIGDDDFSVQLQAELKK KGVAAC	Pesce, F., Newcombe, E. A., Seiffert, P., Tranchant, E. E., Olsen, J. G., Grace, C. R., Kragelund, B. B., & Lindorff-Larsen, K. (2022). Assessment of models for calculating the hydrodynamic radius of intrinsically disordered proteins. Biophysical Journal. https://doi.org/10.1016/j.bpj.2022.12.013
GHR_ICD	59.59	0.38	SKQQRIKMLILPPVPVPKIKGIDPDLLKEGKLEEV NTILAIHDSYKPEFHSDDSWVEFIELDIDEPDEKT EESDTDRLLSSDHEKSHSNLGVKDGDSGRTSCC EPDILETDFNANDIHEGTSEVAQPQRLKGEADLL CLDQKNQNNSPYHDACPATQQPSVIQAEKNKPQ PLPTEGAESTHQAAHIQLSNPSSLSNIDFYAQVS DITPAGSVVLSPGQKNKAGMSQCDMHPEMVSL CQENFLMDNAYFCEADAKKCIPVAPHIKVESHIQ PSLNQEDIYITTESLTTAAGRPGTGEHVPGSEMP VPDYTSIHIVQSPQGLILNATALPLPDKEFLSSCG YVSTDQLNKIMP	Pesce, F., Newcombe, E. A., Seiffert, P., Tranchant, E. E., Olsen, J. G., Grace, C. R., Kragelund, B. B., & Lindorff-Larsen, K. (2022). Assessment of models for calculating the hydrodynamic radius of intrinsically disordered proteins. Biophysical Journal. https://doi.org/10.1016/j.bpj.2022.12.013
NHE6cmdd	32	0.2	GPPLTTTLPACCGPIARCLTSPQAYENQEQLKDD DSDLILNDGDISLTYGDSTVNTEPATSSAPRRFM GNSSEDALDRELAFGDHELVIRGTRLVLPMDDS EPPLNLLDNTRHGPA	Pesce, F., Newcombe, E. A., Seiffert, P., Tranchant, E. E., Olsen, J. G., Grace, C. R., Kragelund, B. B., & Lindorff-Larsen, K. (2022). Assessment of models for calculating the hydrodynamic radius of intrinsically disordered proteins. Biophysical Journal. https://doi.org/10.1016/j.bpj.2022.12.013
ANAC046	36	0.3	NAPSTTITTTKQLSRIDSLDNIDHLLDFSSLPPLID PGFLGQPGPSFSGARQQHDLKPVLHHPTTAPVD	Pesce, F., Newcombe, E. A., Seiffert, P., Tranchant, E. E.,

			NTYLPTQALNFPYHSVHNSGSDFGYGAGSGNN NKGMIKLEHSLVSVSQETGLSSDVNTTATPEISS YPMMMNPAMMDGSKSACDGLDDLIFWEDLYTS	Olsen, J. G., Grace, C. R., Kragelund, B. B., & Lindorff-Larsen, K. (2022). Assessment of models for calculating the hydrodynamic radius of intrinsically disordered proteins. Biophysical Journal. https://doi.org/10.1016/j.bpj.2022.12.013
stath_NTD	9.1	0.3	DSSEEKFLRRIGRFG	Rieloff, E., & Skepö, M. (2020). Phosphorylation of a disordered peptide—Structural effects and force field inconsistencies. Journal of Chemical Theory and Computation. https://pubs.acs.org/doi/abs/10.1021/acs.jctc.9b01190
A1_Aro_minus	27.9	0.8	GSMASASSSQRGRSGSGNSGGGRGGGFGGND NFGRGGNSSGRGGFGGSRGGGGYGGSGDGY NGFGNDGSNSGGGGSSNDFGNYNNQSSNFGP MKGGNFGGRSSGGSGGGGGQYSAKPRNQGGY GGSSSSSSSGSGRRF	Martin, E. W., Holehouse, A. S., Peran, I., Farag, M., Incicco, J. J., Bremer, A., Grace, C. R., Soranno, A., Pappu, R. V., & Mittag, T. (2020). Valence and patterning of aromatic residues determine the phase behavior of prion-like domains. Science, 367(6478), 694–699.
A1_Aro_minus_minus	29.3	0.5	GSMASASSSQRGRSGSGNSGGGRGGGFGGND NSGRGGNSSGRGGFGGSRGGGGSGGSGDGY NGSGNDGSNSGGGGSSNDFGNSNNQSSNSGP MKGGNFGGRSSGGSGGGGGQYSAKPRNQGGS GGSSSSSSSGSGRRS	Martin, E. W., Holehouse, A. S., Peran, I., Farag, M., Incicco, J. J., Bremer, A., Grace, C. R., Soranno, A., Pappu, R. V., & Mittag, T. (2020). Valence and patterning of aromatic residues determine the phase behavior of prion-like domains. Science, 367(6478), 694–699.
A1_Aro_plus	24.2	1.5	GSMAFASSFQRGRYGSGNFGGGRGGGFGGND NFGRGGNFSGRGGFGGSRGGGGYGGSGDGY	Martin, E. W., Holehouse, A. S., Peran, I., Farag, M., Incicco, J.

			NGFGNDGSNFGGGGSYNDFGNYNNQSSNFGP MKGGNFGGRSSGGSYGGGQYFAKPRNQGGYG GSSFSSSYGSGRRF	J., Bremer, A., Grace, C. R., Soranno, A., Pappu, R. V., & Mittag, T. (2020). Valence and patterning of aromatic residues determine the phase behavior of prion-like domains. Science, 367(6478), 694–699.
HeV_PNT3_CTD _200_254	28	0	MSYYHHHHHHHLESTSLYKKAGFTPTEEPPVIPEY YYGSGRRGDLSKSPPRGNVNLDSIKIYTSDDEDE NQLEYEDEF	Nilsson, J. F., Baroudi, H., Gondelaud, F., Pesce, G., Bignon, C., Ptchelkine, D., Chamieh, J., Cottet, H., Kajava, A. V., & Longhi, S. (2022). Molecular Determinants of Fibrillation in a Viral Amyloidogenic Domain from Combined Biochemical and Biophysical Studies. International Journal of Molecular Sciences, 24(1). https://doi.org/10.3390/ijms240 10399
HeV_PNT3_200_ 310_YYY_AAA	40	0	MSYYHHHHHHHLESTSLYKKAGFTPTEEPPVIPEA AAGSGRRGDLSKSPPRGNVNLDSIKIYTSDDEDE NQLEYEDEFAKSSSEVVIDTTPEDNDSINQEEVV GDPSDQGLEHPFPLGKFPEKEETPDVRRKDS	Nilsson, J. F., Baroudi, H., Gondelaud, F., Pesce, G., Bignon, C., Ptchelkine, D., Chamieh, J., Cottet, H., Kajava, A. V., & Longhi, S. (2022). Molecular Determinants of Fibrillation in a Viral Amyloidogenic Domain from Combined Biochemical and Biophysical Studies. International Journal of Molecular Sciences, 24(1). https://doi.org/10.3390/ijms240 10399
HeV_PNT3_200_ 310_WT	37	0	MSYYHHHHHHHLESTSLYKKAGSTPTEEPPVIPEY YYGSGRRGDLSKSPPRGNVNLDSIKIYTSDDEDE NQLEYEDEFAKSSSEVVIDTTPEDNDSINQEEVV GDPSDQGLEHPFPLGKFPEKEETPDVRRKDS	Nilsson, J. F., Baroudi, H., Gondelaud, F., Pesce, G., Bignon, C., Ptchelkine, D., Chamieh, J., Cottet, H., Kajava,

				A. V., & Longhi, S. (2022). Molecular Determinants of Fibrillation in a Viral Amyloidogenic Domain from Combined Biochemical and Biophysical Studies. International Journal of Molecular Sciences, 24(1). https://doi.org/10.3390/ijms240 10399
NiV_PNT3_200_3 14_WT	37	0	MSYYHHHHHHLESTSLYKKAGFDPAKDSPVIAE HYYGLGVKEQNVGPQTSRNVNLDSIKLYTSDDE EADQLEFEDEFAGSSSEVIVGISPEDEEPSSVGG KPNESIGRTIEGQSIRDNLQAKDNKSTDVPGAGP KDS	Nilsson, J. F., Baroudi, H., Gondelaud, F., Pesce, G., Bignon, C., Ptchelkine, D., Chamieh, J., Cottet, H., Kajava, A. V., & Longhi, S. (2022). Molecular Determinants of Fibrillation in a Viral Amyloidogenic Domain from Combined Biochemical and Biophysical Studies. International Journal of Molecular Sciences, 24(1). https://doi.org/10.3390/ijms240 10399
red1_288_345	25	0	GAMGISLPLLKQDDWLSSSKPFGSSTPNVVIEFD SDDDGDDFSNSKIEQSNLEKPPSNSENGGSHHH HHH	TBD
p150L_342_475	41	0	MAERLGKQLKLRAEREEKEKLKEEAKRAKEEAK KKKEEEKELKEKERREKREKDEKEKAEKQRLKE ERRKERQEALEAKLEEKRKKEEEKRLREEEKRIK AEKAEITRFFQKPKTPQAPKTLAGSCGKFAPFEIK ELEHHHHHH	Gopinathan Nair, A., Rabas, N., Lejon, S., Homiski, C., Osborne, M. J., Cyr, N., Sverzhinsky, A., Melendy, T., Pascal, J. M., Laue, E. D., Borden, K. L. B., Omichinski, J. G., & Verreault, A. (2022). Unorthodox PCNA Binding by Chromatin Assembly Factor 1. International Journal of Molecular Sciences, 23(19).

				https://doi.org/10.3390/ijms231911099
E1A_2022	36	0	GSMSHFEPPTLHELYDLDVTAPEDPNEEAVSQIFPDSVMLAVQEGIDLLTFPPAPGSPEPPHLSRQPEQPEQRALGPVSMPNLVPEVIDLYCYEQLNPPSDDEDEEGEEFVLDY	González-Foutel, N. S., Glavina, J., Borcherds, W. M., Safranchik, M., Barrera-Vilarmau, S., Sagar, A., Estaña, A., Barozet, A., Garrone, N. A., Fernandez-Ballester, G., Blanes-Mira, C., Sánchez, I. E., de Prat-Gay, G., Cortés, J., Bernadó, P., Pappu, R. V., Holehouse, A. S., Daughdrill, G. W., & Chemes, L. B. (2022). Conformational buffering underlies functional selection in intrinsically disordered protein regions. Nature Structural & Molecular Biology, 29(8), 781–790.
RelA_TAD	27	0	MGSVPKPAPQPYTFPASLSTINFDEFSPMLLPSGQISNQALALAPSSAPVLAQTMVPSSAMVPLAQPPAPAPVLTPGPPQSLSAPVPKSTQAGEGTLSEALLHLQFDADEDLGALLGNSTDPGVFTDLASVDNSEFQQLLNQGVSMSHSTAEPMLMEYPEAITRLVTGSQRPPDPAPTPLGTSGLPNGLSGDEDFSSIADMDFSALLSQISSLEHHHHHH	Baughman, H. E. R., Narang, D., Chen, W., Villagrán Suárez, A. C., Lee, J., Bachochin, M. J., Gunther, T. R., Wolynes, P. G., & Komives, E. A. (2022). An intrinsically disordered transcription activation domain increases the DNA binding affinity and reduces the specificity of NFκB p50/RelA. The Journal of Biological Chemistry, 298(9), 102349.
EIF_450_1_249	52	0	GSMTDETAHPTQSASKQESAALKQTGDDQQESQQQRGYTNYNNGSNYTQKKPYNSNRPHQQRGGKFGPNRYNNRGNYNGGGSFRGGHMGANSSNVPWTGYYNNYPVYYQPQQMAAAGSAPANPIPVEEKSPVPTKIEITTKSGEHLDLKEQHKAKLQSQERSTVSPQPESKLKETSDSTSTSTPTPTPSTNDSKASSEENISEAEKTRRNFIEQVKLRKAALEKKRKEQLEGSSGNNNIPMKTTPENVEEK	Chaves-Arquero, B., Martínez-Lumbreras, S., Sibille, N., Camero, S., Bernadó, P., Jiménez, M. Á., Zorrilla, S., & Pérez-Cañadillas, J. M. (2022). eIF4G1 N-terminal intrinsically disordered domain is a multi-docking station for RNA, Pab1,

				Pub1, and self-assembly. Frontiers in Molecular Biosciences, 9, 986121.
TIF2_624_774	37	0	ERADGQSRLHDSKGQTKLLQLLTTKSDQMEPSP LASSLSDTNKDSTGSLPGSGSTHGTSLKEKHKIL HRLLQDSSSPVDLAKLTAEATGKDLSQESSSTAP GSEVTIKQEPVSPKKKENALLRYLLDKDDTKDIGL PEITPKLERLDSKT	Senicourt, L., le Maire, A., Allemand, F., Carvalho, J. E., Guee, L., Germain, P., Schubert, M., Bernadó, P., Bourguet, W., & Sibille, N. (2021). Structural insights into the interaction of the intrinsically disordered co-activator TIF2 with retinoic acid receptor heterodimer (RXR/RAR). Journal of Molecular Biology, 433(9), 166899.
IR_CTD	38	0	GPRRNQPAEQTTTTTTHTVVQQQTGGNTPAQG GTDATRAEDASLNRRDSQGSVASTHWSDSSSE VVNPYAEVGGARNSLSAHQPEEHIYDEVAADPG YSVIQNFSGSGPVTGRLIGTPGQGIQSTYALLAN SGGLRLGMGGLTSGGESAVSSVNAAPTPGPVR FVWSHPQFEK	TBD
Tau_ht35_2022	46	0	EPPKSGDRSGYSSPGSPGTPGSRSRTPSLPTPP TREPKKVAVVRTPPKSPSSAKSRLQTAPVPMPD LKNVKSKIGSTENLKHQPGGGKVQIINKKLDLSN VQSKCGSKDNIKHVPGGGSVQIVYKPVDLSKVT SKCGSLGNIHHKPGGGQVEVKSEKLDFKDRVQS KIGSLDNITHVPGGGNKKIETHKLTFRENAKAKTD HGAEIVYKSPVVSGDTSPRHLSNVSSTGSIDMVD SPQLATLADEVSASLAKQGL	Lyu, C., Da Vela, S., Al-Hilaly, Y., Marshall, K. E., Thorogate, R., Svergun, D., Serpell, L. C., Pastore, A., & Hanger, D. P. (2021). The Disease Associated Tau35 Fragment has an Increased Propensity to Aggregate Compared to Full-Length Tau. Frontiers in Molecular Biosciences, 8, 779240.
Tau_ht410_2N3R	63	0	MAEPRQEFEVMEDHAGTYGLGDRKDQGGYTM HQDQEGDTDAGLKESPLQTPTEDGSEEPGSETS DAKSTPTAEDVTAPLVDEGAPGKQAAAQPHTEIP EGTTAEEAGIGDTPSLEDEAAGHVTQARMVSKS	Lyu, C., Da Vela, S., Al-Hilaly, Y., Marshall, K. E., Thorogate, R., Svergun, D., Serpell, L. C., Pastore, A., & Hanger, D. P.

			KDGTGSDDKKAKGADGKTKIATPRGAAPPGQKG QANATRIPAKTPPAPKTPPSSGEPPKSGDRSGY SSPGSPGTPGSRSRTPSLPTPPTREPKKVAVVR TPPKSPSSAKSRLQTAPVPMPDLKNVKSKIGSTE NLKHQPGGGKVQIVYKPVDLSKVTSKCGSLGNIH HKPGGGQVEVKSEKLDFKDRVQSKIGSLDNITHV PGGGNKKIETHKLTFRENAKAKTDHGAEIVYKSP VVSGDTSPRHLSNVSSTGSIDMVDSPQLATLAD EVSASLAKQGL	(2021). The Disease Associated Tau35 Fragment has an Increased Propensity to Aggregate Compared to Full-Length Tau. Frontiers in Molecular Biosciences, 8, 779240.
Tau_ht410_2N4R	67	0	MAEPRQEFEVMEDHAGTYGLGDRKDQGGYTM HQDQEGDTDAGLKESPLQTPTEDGSEEPGSETS DAKSTPTAEDVTAPLVDEGAPGKQAAAQPHTEIP EGTTAEEAGIGDTPSLEDEAAGHVTQARMVSKS KDGTGSDDKKAKGADGKTKIATPRGAAPPGQKG QANATRIPAKTPPAPKTPPSSGEPPKSGDRSGY SSPGSPGTPGSRSRTPSLPTPPTREPKKVAVVR TPPKSPSSAKSRLQTAPVPMPDLKNVKSKIGSTE NLKHQPGGGKVQIINKKLDLSNVQSKCGSKDNIK HVPGGGSVQIVYKPVDLSKVTSKCGSLGNIHHKP GGGQVEVKSEKLDFKDRVQSKIGSLDNITHVPG GGNKKIETHKLTFRENAKAKTDHGAEIVYKSPVV SGDTSPRHLSNVSSTGSIDMVDSPQLATLADEV SASLAKQGL	Lyu, C., Da Vela, S., Al-Hilaly, Y., Marshall, K. E., Thorogate, R., Svergun, D., Serpell, L. C., Pastore, A., & Hanger, D. P. (2021). The Disease Associated Tau35 Fragment has an Increased Propensity to Aggregate Compared to Full-Length Tau. Frontiers in Molecular Biosciences, 8, 779240.
SMAD_linker	29	0	GPLPPVLVPRHTEILTELPPLDDYTHSIPENTNFP AGIEPQSNYIPETPPPGYISEDGETSDQQLNQSM DTGSPAELSPTTLSPVNHSLD	Gomes, T., Martin-Malpartida, P., Ruiz, L., Aragón, E., Cordeiro, T. N., & Macias, M. J. (2021). Conformational landscape of multidomain SMAD proteins. Computational and Structural Biotechnology Journal, 19, 5210–5224.
MenV_LBD	25	0	TTIKIMDPGVGDGATAAKSKRLFKEAPVVVSGPVI GDNPIVDADTIQLDELARPSLPKTKSQ	Webby, M. N., Herr, N., Bulloch, E. M. M., Schmitz, M., Keown, J. R., Goldstone, D. C., & Kingston, R. L. (2021). Structural Analysis of the Menangle Virus P Protein Reveals a Soft Boundary between Ordered and

				Disordered Regions. Viruses, 13(9). https://doi.org/10.3390/v1309173 7
syndecan3_ED	65	0	MGSSHHHHHHSSGLVPRGSMAQRWRSENFER PVDLEGSGDDDSFPDDELDDLYSGSGSGYFEQ ESGIETAMETRFSPDVALAVSTTPAVLPTTNIQPV GTPFEELPSERPTLEPATSPLVVTEVPEEPSQRA TTVSTTMETATTAATSTGDPTVATVPATVATATP STPAAPPFTATTAVIRTTGVRRLLPLPLTTVATAR ATTPEAPSPPTTAAVLDTEAPTPRLVSTATSRPR ALPRPATTQEPDIPERSTLPLGTTAPGPTEVAQT PTPETFLTTIRDEPEVPVSGGPSGDFELPEEETT QPDTANEVVAVGGAAAKASSPPGTLPKGARPGP GLLDNAIDSGSSAAQLPQKSILERKEVLVDYKDD DDK	Gondelaud, F., Bouakil, M., Le Fèvre, A., Miele, A. E., Chirot, F., Duclos, B., Liwo, A., & Ricard-Blum, S. (2021). Extended disorder at the cell surface: The conformational landscape of the ectodomains of syndecans. Matrix Biology Plus, 12, 100081.
syndecan4	42	0	GSSHHHHHHSSGLVPRGSHMESIRETEVIDPQD LLEGRYFSGALPDDEDVVGPGQESDDFELSGSG DLDDLEDSMIGPEVVHPLVPLDNHIPERAGSGSQ VPTEPKKLEENEVIPKRISPVEESEDVSNKVSMS STVQGSNIFERTEVLAGCPEHDYKDDDDK	Gondelaud, F., Bouakil, M., Le Fèvre, A., Miele, A. E., Chirot, F., Duclos, B., Liwo, A., & Ricard-Blum, S. (2021). Extended disorder at the cell surface: The conformational landscape of the ectodomains of syndecans. Matrix Biology Plus, 12, 100081.
N_FATZ_1	35	0	MAHHHHHHVDDDDKIMPLSGTPAPNKKRKSSKL IMELTGGGQESSGLNLGKKISVPRDVMLEELSLL TNRGSKMFKLRQMRVEKFIYENHPDVFSDSSMD HFQKFLPTVGGQLGTAGQGFSYSKSNGRGGSQ AGGSGSAGQYGSDQQHHLGSGSGAGGTGGPA GQAGRGGAAGTAGVGETGSGDQAGGEAE	Sponga, A., Arolas, J. L., Schwarz, T. C., Jeffries, C. M., Rodriguez Chamorro, A., Kostan, J., Ghisleni, A., Drepper, F., Polyansky, A., De Almeida Ribeiro, E., Pedron, M., Zawadzka-Kazimierczuk, A., Mlynek, G., Peterbauer, T., Doto, P., Schreiner, C., Hollerl, E., Mateos, B., Geist, L., … Djinović-Carugo, K. (2021). Order from disorder in the sarcomere: FATZ forms a fuzzy but tight complex and phase-

				separated condensates with α-actinin. Science Advances, 7(22). https://doi.org/10.1126/sciadv.abg7653
DeltaN_FATZ_1	39	0	GPTVGGQLGTAGQGFSYSKSNGRGGSQAGGS GSAGQYGSDQQHHLGSGSGAGGTGGPAGQAG RGGAAGTAGVGETGSGDQAGGEGKHITVFKTYI SPWERAMGVDPQQKMELGIDLLAYGAKAELPKY KSFNRTAMPYGGYEKASKRMTFQMPKFDLGPLL SEPLVLYNQNLSNRPSFNRTPIPWLSSGEPVDY NVDIGIPLDGETEEL	Sponga, A., Arolas, J. L., Schwarz, T. C., Jeffries, C. M., Rodriguez Chamorro, A., Kostan, J., Ghisleni, A., Drepper, F., Polyansky, A., De Almeida Ribeiro, E., Pedron, M., Zawadzka-Kazimierczuk, A., Mlynek, G., Peterbauer, T., Doto, P., Schreiner, C., Hollerl, E., Mateos, B., Geist, L., … Djinović-Carugo, K. (2021). Order from disorder in the sarcomere: FATZ forms a fuzzy but tight complex and phase-separated condensates with α-actinin. Science Advances, 7(22). https://doi.org/10.1126/sciadv.abg7653
histatin_2021	15	0	DSHAKRHHGYKRKFHEKHHSHRGY	Sagar, A., Jeffries, C. M., Petoukhov, M. V., Svergun, D. I., & Bernadó, P. (2021). Comment on the Optimal Parameters to Derive Intrinsically Disordered Protein Conformational Ensembles from Small-Angle X-ray Scattering Data Using the Ensemble Optimization Method. Journal of Chemical Theory and Computation, 17(4), 2014–2021.
synthELP	66	0	GGVPGAIPGGVPGGVFYPGAGLGALGGGALGP GGKPLKPVPGGLAGAGLGAGLGAFPAVTFPGAL	Lockhart-Cairns, M. P., Newandee, H., Thomson, J.,

			VPGGVADAAAAYKAAKAGAGLGGVPGVGGLGV SAGAVVPQPGAGVKPGKVPGVGLPGVYPGGVL PGARFPGVGVLPGVPTGAGVKPKAPGVGGAFA GIPGVGPFGGPQPGVPLGYPIKAPKLPGGYGLP YTTGKLPYGYGPGGVAGAAGKAGYPTGTGVGP QAAAAAAAKAAAKFGAGAAGVLPGVGGAGVPG VPGAIPGIGGIAGVGTPAAAAAAAAAAKAAKYGA AAGLVPGGPGFGPGVVGVPGAGVPGVGVPGAG IPVVPGAGIPGAAVPGVVSPEAAAKAAAKAAKYG ARPGVGVGGIPTYGVGAGGFPGFGVGVGGIPG VAGVPGVGGVPGVGGVPGVGISPEAQAAAAAK AAKYGVGTPAAAAAKAAAKAAQFGLVPGVGVAP GVGVAPGVGVAPGVGLAPGVGVAPGVGVAPGV GVAPGIGPGGVAAAAKSAAKVAAKAQLRAAAGL GAGIPGLGVGVGVPGLGVGAGVPGLGVGAGVP GFGAVPGALAAAKAAKYGAAVPGVLGGLGALGG VGIPGGVVGAGPAAAAAAAKAAAKAAQFGLVGA AGLGGLGVGGLGVPGVGGLGGIPPAAAAKAAKY GAAGLGGVLGGAGQFPLGGVAARPGFGLSPIFP GGACLGKACGRKRK	Weiss, A. S., Baldock, C., & Tarakanova, A. (2020). Transglutaminase-mediated cross-linking of tropoelastin to fibrillin stabilises the elastin precursor prior to elastic fibre assembly. Journal of Molecular Biology, 432(21), 5736–5751.
UL11	24	0	MGLSFSGTRPCCCRNNVLITDDGEVVSLTAHDF DVVDIESEEEGNFYVPPDMRGVTRAPGRQRLRS SDPPSRHTHRRTPGGACPATQFPPPMSDSEWS HPQFEK	Metrick, C. M., Koenigsberg, A. L., & Heldwein, E. E. (2020). Conserved Outer Tegument Component UL11 from Herpes Simplex Virus 1 Is an Intrinsically Disordered, RNA-Binding Protein. mBio, 11(3). https://doi.org/10.1128/mBio.00 810-20
GON7_NTD	31	0	MGHHHHHHENLYFQGELLGEYVGQEGKPQKLR VSCEAPGDGDPFQGLLSGVAQMKDMVTELFDP LVQGEVQHRVAAAPDEDLDGDDEDDAEDENNID NRTNFDGPSAKRPKTPS	Arrondel, C., Missoury, S., Snoek, R., Patat, J., Menara, G., Collinet, B., Liger, D., Durand, D., Gribouval, O., Boyer, O., Buscara, L., Martin, G., Machuca, E., Nevo, F., Lescop, E., Braun, D. A., Boschat, A.-C., Sanquer, S., Guerrera, I. C., … Mollet, G. (2019). Defects in t6A tRNA modification due to GON7 and YRDC mutations lead to

				Galloway-Mowat syndrome. Nature Communications, 10(1), 3967.
Bmal1_CTD_P62 4A	28	0	GPDASSPGGKKILNGGTPDIPSTGLLPGQAQETP GYPYSDSSSILGENPHIGIDMIDNDQGSSSPSND EAAMAVIMSLLEADAGLGGPVDFSDLPWAL	Garg, A., Orru, R., Ye, W., Distler, U., Chojnacki, J. E., Köhn, M., Tenzer, S., Sönnichsen, C., & Wolf, E. (2019). Structural and mechanistic insights into the interaction of the circadian transcription factor BMAL1 with the KIX domain of the CREB-binding protein. The Journal of Biological Chemistry, 294(45), 16604–16619.
NID_2059_2325	47	0	GPHMQVPRTHRLITLADHICQIITQDFARNQVPS QASTSTFQTSPSALSSTPVRTKTSSRYSPESQS QTVLHPRPGPRVSPENLVDKSRGSRPGKSPERS HIPSEPYEPISPPQGPAVHEKQDSMLLLSQRGVD PAEQRSDSRSPGSISYLPSFFTKLESTSPMVKSK KQEIFRKLNSSGGGDSDMAAAQPGTEIFNLPAVT TSGAVSSRSHSFADPASNLGLEDIIRKALMGSFD DKVEDHGVVMSHPVGIMPGSASTSVVTSSEARR DE	Cordeiro, T. N., Sibille, N., Germain, P., Barthe, P., Boulahtouf, A., Allemand, F., Bailly, R., Vivat, V., Ebel, C., Barducci, A., Bourguet, W., le Maire, A., & Bernadó, P. (2019). Interplay of protein disorder in retinoic acid receptor heterodimer and its corepressor regulates gene expression. Structure , 27(8), 1270–1285.e6.
MAP2c	67	0	MADERKDEGKAPHWTSASLTEAAAHPHSPEMK DQGGSGEGLSRSANGFPYREEEEGAFGEHGSQ GTYSDTKENGINGELTSADRETAEEVSARIVQVV TAEAVAVLKGEQEKEAQHKDQPAALPLAAEETV NLPPSPPPSPASEQTAALEEATSGESAQAPSAF KQAKDKVTDGITKSPEKRSSLPRPSSILPPRRGV SGDREENSFSLNSSISSARRTTRSEPIRRAGKSG TSTPTTPGSTAITPGTPPSYSSRTPGTPGTPSYP RTPGTPKSGILVPSEKKVAIIRTPPKSPATPKQLR LINQPLPDLKNVKSKIGSTDNIKYQPKGGQVQIVT KKIDLSHVTSKCGSLKNIRHRPGGGRVKIESVKL DFKEKAQAKVGSLDNAHHVPGGGNVKIDSQKLN	Melková, K., Zapletal, V., Jansen, S., Nomilner, E., Zachrdla, M., Hritz, J., Nováček, J., Zweckstetter, M., Jensen, M. R., Blackledge, M., & Žídek, L. (2018). Functionally specific binding regions of microtubule-associated protein 2c exhibit distinct conformations and dynamics. The Journal of Biological Chemistry, 293(34), 13297–13309.

			FREHAKARVDHGAEIITQSPSRSSVASPRRLSNV SSSGSINLLESPQLATLAEDVTAALAKQGL	
TRF2_BR	17	0	GPPGSMAGGGGSSDGSGRAAGRRASRSSGRA RRGRHEPGLGGPAERGAG	Necasová, I., Janoušková, E., Klumpler, T., & Hofr, C. (2017). Basic domain of telomere guardian TRF2 reduces D-loop unwinding whereas Rap1 restores it. Nucleic Acids Research, 45(21), 12170–12180.

SUPPLEMENTARY REFERENCES

(1)   Lalmansingh, J. M.; Keeley, A. T.; Ruff, K. M.; Pappu, R. V.; Holehouse, A. S. SOURSOP: A Python Package for the Analysis of Simulations of Intrinsically Disordered Proteins. bioRxiv 2023. https://doi.org/10.1101/2023.02.16.528879.

(2)   Holehouse, A. S.; Garai, K.; Lyle, N.; Vitalis, A.; Pappu, R. V. Quantitative Assessments of the Distinct Contributions of Polypeptide Backbone Amides versus Side Chain Groups to Chain Expansion via Chemical Denaturation. J. Am. Chem. Soc. 2015, 137 (8), 2984–2995.

(3)   Rubinstein, M.; Colby, R. H. Polymer Physics; Oxford University Press: New York, 2003.

(4)   Martin, E. W.; Holehouse, A. S.; Grace, C. R.; Hughes, A.; Pappu, R. V.; Mittag, T. Sequence Determinants of the Conformational Properties of an Intrinsically Disordered Protein Prior to and upon Multisite Phosphorylation. J. Am. Chem. Soc. 2016, 138 (47), 15323–15335.

(5)   Holehouse, A. S.; Sukenik, S. Controlling Structural Bias in Intrinsically Disordered Proteins Using Solution Space Scanning. J. Chem. Theory Comput. 2020, 16 (3), 1794–1805.

(6)   Das, R. K.; Huang, Y.; Phillips, A. H.; Kriwacki, R. W.; Pappu, R. V. Cryptic Sequence Features within the Disordered Protein p27Kip1 Regulate Cell Cycle Signaling. Proc. Natl. Acad. Sci. U. S. A. 2016, 113 (20), 5616–5621.

(7)   Sherry, K. P.; Das, R. K.; Pappu, R. V.; Barrick, D. Control of Transcriptional Activity by Design of Charge Patterning in the Intrinsically Disordered RAM Region of the Notch Receptor. Proc. Natl. Acad. Sci. U. S. A. 2017, 114 (44), E9243–E9252.

(8)   Martin, E. W.; Holehouse, A. S.; Peran, I.; Farag, M.; Incicco, J. J.; Bremer, A.; Grace, C. R.; Soranno, A.; Pappu, R. V.; Mittag, T. Valence and Patterning of Aromatic Residues Determine the Phase Behavior of Prion-like Domains. Science 2020, 367 (6478), 694–699.

(9)   Robustelli, P.; Piana, S.; Shaw, D. E. Developing a Molecular Dynamics Force Field for Both Folded and Disordered Protein States. Proc. Natl. Acad. Sci. U. S. A. 2018, 115 (21), E4758–E4766.

(10)   Holehouse, A. S.; Das, R. K.; Ahad, J. N.; Richardson, M. O. G.; Pappu, R. V. CIDER: Resources to Analyze Sequence-Ensemble Relationships of Intrinsically Disordered Proteins. Biophys. J. 2017, 112 (1), 16–21.

(11)   O'Brien, E. P.; Morrison, G.; Brooks, B. R.; Thirumalai, D. How Accurate Are Polymer Models in the Analysis of Forster Resonance Energy Transfer Experiments on Proteins? J. Chem. Phys. 2009, 130 (12), 124903.

(12)   Zheng, W.; Zerze, G. H.; Borgia, A.; Mittal, J.; Schuler, B.; Best, R. B. Inferring Properties of Disordered Chains from FRET Transfer Efficiencies. J. Chem. Phys. 2018, 148 (12), 123329.